Disc–jet coupling in low-luminosity accreting neutron stars

V. Tudor,[1]⋆ J. C. A. Miller-Jones,[1] A. Patruno,[2,3] C. R. D'Angelo,[2] P. G. Jonker,[4,5]
D. M. Russell,[6] T. D. Russell,[1,7] F. Bernardini,[6] F. Lewis,[8,9] A. T. Deller,[10]
J. W. T. Hessels,[3,7] S. Migliari,[11,12] R. M. Plotkin,[1] R. Soria[1] and R. Wijnands[7]

[1]*International Centre for Radio Astronomy Research – Curtin University, GPO Box U1987, Perth, WA 6845, Australia*
[2]*Leiden Observatory, Leiden University, PO Box 9513, NL-2300 RA Leiden, the Netherlands*
[3]*ASTRON, the Netherlands Institute for Radio Astronomy, Postbus 2, NL-7990 AA Dwingeloo, the Netherlands*
[4]*SRON, Netherlands Institute for Space Research, Sorbonnelaan 2, NL-3584 CA Utrecht, the Netherlands*
[5]*Department of Astrophysics/IMAPP, Radboud University, PO Box 9010, NL-6500 GL Nijmegen, the Netherlands*
[6]*New York University Abu Dhabi, PO Box 129188, Abu Dhabi, UAE*
[7]*Anton Pannekoek Institute for Astronomy, University of Amsterdam, PO Box 94249, NL-1090 GE Amsterdam, the Netherlands*
[8]*Faulkes Telescope Project, School of Physics and Astronomy, Cardiff University, The Parade, Cardiff CF24 3AA, UK*
[9]*Astrophysics Research Institute, Liverpool John Moores University, 146 Brownlow Hill, Liverpool L3 5RF, UK*
[10]*Centre for Astrophysics and Supercomputing, Swinburne University of Technology, PO Box 218, Hawthorn, VIC 3122, Australia*
[11]*European Space Astronomy Centre (ESAC), E-28692 Villanueva de la Cañada, Madrid, Spain*
[12]*Department of Quantum Physics and Astrophysics & Institute of Cosmos Sciences, University of Barcelona, E-08028 Barcelona, Spain*

ABSTRACT

In outburst, neutron star X-ray binaries produce less powerful jets than black holes at a given X-ray luminosity. This has made them more difficult to study as they fade towards quiescence. To explore whether neutron stars power jets at low accretion rates ($L_X \lesssim 10^{36}$ erg s^{-1}), we investigate the radio and X-ray properties of three accreting millisecond X-ray pulsars (IGR J17511−3057, SAX J1808.4−3658 and IGR J00291+5934) during their outbursts in 2015, and of the non-pulsing neutron star Cen X−4 in quiescence (2015) and in outburst (1979). We did not detect the radio counterpart of IGR J17511−3057 in outburst or of Cen X−4 in quiescence, but did detect IGR J00291+5934 and SAX J1808.4−3658, showing that at least some neutron stars launch jets at low accretion rates. While the radio and X-ray emission in IGR J00291+5934 seem to be tightly correlated, the relationship in SAX J1808.4−3658 is more complicated. We find that SAX J1808.4−3658 produces jets during the reflaring tail, and we explore a toy model to ascertain whether the radio emission could be attributed to the onset of a strong propeller. The lack of a universal radio/X-ray correlation, with different behaviours in different neutron star systems (with various radio/X-ray correlations; some being radio faint and others not), points at distinct disc–jet interactions in individual sources, while always being fainter in the radio band than black holes at the same X-ray luminosity.

Key words: accretion, accretion discs – stars: neutron – radio continuum: transients – ISM: jets and outflows – X-rays: binaries.

1 INTRODUCTION

Radio jets are a common feature among accreting compact objects, most prominently associated with black holes (e.g. Mirabel & Rodríguez 1994), but also produced by neutron stars (Fomalont, Geldzahler & Bradshaw 2001) and white dwarfs (Coppejans et al. 2015). Similar to black holes, neutron star X-ray binaries have been found to produce both resolved and compact radio jets (Fender et al. 2004c; Migliari et al. 2010; Miller-Jones et al. 2010; Spencer

et al. 2013), albeit at a fainter radio luminosity than black holes at the same X-ray luminosity in the hard state (a factor of ≈30; Migliari & Fender 2006), when the X-ray spectrum is dominated by a hard power-law component (van Paradijs 1998).

Despite a long history of observations, it is still unknown how jets are launched. Comparing different classes of accreting objects will provide clues regarding which jet properties are universal, and which rely on the nature of the compact object. For example, comparing neutron star and black hole jets can help to distinguish between different jet models and jet launching mechanisms. Possibilities include the Blandford–Payne model (whereby the jet is produced by the collimation of disc winds by the magnetic fields

⋆ E-mail: vlad.tudor@postgrad.curtin.edu.au

in the disc, and is possible in both neutron stars and black holes; Blandford & Payne 1982), the Blandford–Znajek model (in which the jet is launched by the magnetic field of the disc, extracting angular momentum from the ergosphere of a spinning black hole; Blandford & Znajek 1977) or models powered by the spin of a neutron star, such as the X-wind model (initially developed for young stellar objects, Shu et al. 1994; but potentially applicable to neutron stars, Migliari & Fender 2006; Migliari et al. 2012).

One way to compare neutron star and black hole jets is through investigations of their disc–jet coupling. The connection between inflow (disc) and outflow (jets) processes is manifested in the empirical radio – X-ray luminosity correlation of hard-state black hole X-ray binaries, which links the radio luminosity (set by the jet power) with the X-ray luminosity (a proxy for the mass accretion rate through the inner regions of the accretion flow; Fender, Gallo & Jonker 2003). This relationship takes the form of a power law between the radio and X-ray luminosities, $L_R \propto L_X^\beta$, where $\beta \approx 0.5$–0.7 in the most well-studied black hole sources such as GX 339–4 or V404 Cygni (Corbel et al. 2000; Gallo, Fender & Pooley 2003; Corbel et al. 2013; Gallo et al. 2014; Plotkin et al. 2017).

Knowledge of the difference between the radio emission of neutron stars and black holes can also be used to determine the nature of the accreting compact object in new transient or quiescent systems. The three ways of irrefutably distinguishing between neutron stars and black holes are the detection of Type I X-ray bursts (Joss 1977) or coherent X-ray pulsations (Lamb, Pethick & Pines 1973), which both imply that the compact object is a neutron star, or the measurement of the mass function of the system in question (Casares 2007). Due to the low brightness of donor stars, and the large distances and high extinctions typical of X-ray binaries, mass functions can often be very difficult to measure. So, in the absence of Type I bursts or pulsations, it is difficult to identify the nature of the accretor. One promising approach is through simultaneous radio and X-ray observations, especially since radio facilities have reached the requisite sensitivity to detect an increasing number of X-ray binaries (e.g. the Karl G. Jansky Very Large Array; Perley et al. 2011), and to track the closest systems as they decay back towards quiescence.

Transient X-ray binaries undergo outbursts in which their X-ray luminosities increase by up to six orders of magnitude over their quiescent levels, accompanied by spectral changes and strong outflows. As radio jets from black hole X-ray binaries in outburst are bright, a factor of at least 30 louder than those of 'ordinary' neutron stars (Migliari & Fender 2006), it has been possible to study the radio–X-ray correlation for black holes over eight orders of magnitude in X-ray luminosity. As systems change luminosities in the hard state as they decay towards quiescence on week to month time-scales, inflow–outflow coupling can be directly traced in individual sources (Corbel, Koerding & Kaaret 2008; Coriat et al. 2011; Corbel et al. 2013; Plotkin et al. 2017).

Gallo et al. (2014) found that the radio–X-ray correlations of individual black hole systems have less scatter than the black hole X-ray binary population as a whole. Different correlation slopes β in different sources suggest different, or evolving, radiative efficiencies (Heinz & Sunyaev 2003). Above $L_X \approx 10^{36}$ erg s^{-1}, a few black hole X-ray binaries are seen to follow a steeper ($\beta \approx 1.4$), radiatively efficient track in the radio/X-ray plane (Coriat et al. 2011). As they become fainter, the radiatively efficient systems that have been observed long enough are seen to switch to the primary, radiatively inefficient track with $\beta \approx 0.7$ (H 1743−322, Jonker et al. 2010; MAXI J1659−152, Jonker et al. 2012; XTE J1752−223, Ratti et al. 2012). Gallo et al. (2014), however, did not find strong statistical evidence for the existence of two tracks in the overall black hole population, meaning that individual sources could follow different tracks.

In comparison to black holes, the inflow–outflow connection in neutron stars is complicated by the presence of a crust, a magnetosphere and possibly other as-yet unknown factors. Specifically, the crust prevents accreted material from reaching an ergosphere, the magnetic field can alter or halt the accretion flow and outflows through mechanisms that do not operate for black holes (such as the propeller effect; Illarionov & Sunyaev 1975). In addition, due to their less luminous jets, a narrower range of radio luminosities is accessible for neutron stars before telescope sensitivity limits are reached. Because of this, neutron star jets have been less well explored to date, with few reported radio detections for systems below $L_X \approx 10^{36}$ erg s^{-1}.

In the case of black holes, the radio–X-ray correlation is only seen in the hard and quiescent X-ray states. In the soft state, at higher accretion rates, when the spectrum is dominated by a soft, thermal component, steady jets are suppressed in black holes (Fender, Belloni & Gallo 2004a) and some neutron stars (Migliari et al. 2003; Tudose et al. 2009; Miller-Jones et al. 2010; Migliari 2011), although Migliari et al. (2004) present two radio detections of a neutron star in the soft state. The analogous low-luminosity, hard-state neutron star systems are the atoll sources [ordinary neutron stars that are typically accreting at 1–10 per cent the Eddington luminosity (L_{Edd}); Muno, Remillard & Chakrabarty 2002], accreting millisecond pulsars (AMXPs) and transitional millisecond pulsars (tMSPs). In the context of the 'recycling' scenario (Bisnovatyi-Kogan & Komberg 1974; Alpar et al. 1982; Radhakrishnan & Srinivasan 1982), AMXPs and tMSPs are thought to be missing links between radio millisecond pulsars and neutron star X-ray binaries. AMXPs display X-ray pulsations at the spin period of the neutron star (Wijnands & van der Klis 1998), whereas tMSPs switch between an accreting state, when the system is observed as an X-ray binary, and a non-accreting state, when the neutron star becomes a radio millisecond pulsar (Archibald et al. 2009). The tMSP M28I behaved as an AMXP in outburst (Papitto et al. 2013), and the tMSPs PSR J1023+0038 (Archibald et al. 2015) and XSS J12270−4859 (Papitto et al. 2015) exhibit coherent X-ray pulsations akin to AMXPs, so tMSPs may in fact be a subset of AMXPs. So far, studies hint at diverse disc–jet coupling relations for different neutron stars, as described below.

The first studies that showed disc–jet coupling in neutron stars focused on sources that persistently accrete close to the Eddington luminosity. Their radio emission appeared to correlate with the spectral state of the source (Penninx et al. 1988; Hjellming et al. 1990a,b). Migliari et al. (2003) later found other evidence for disc–jet coupling in the source 4U 1728−34, which follows a relationship of the form $L_R \propto L_X^{1.5\pm0.2}$, as theoretically predicted for radiatively efficient accretion flows. Migliari & Fender (2006) extended their sample with three additional atolls in the hard state, which, as a sample, displayed a similar $\beta \approx 1.4$ relationship. In addition, they also added four AMXPs to their sample, showing that AMXPs are more scattered on the radio–X-ray luminosity plane, and can reach slightly higher radio luminosities than atoll sources at similar X-ray luminosities. Later, the atoll source Aql X−1 was found to follow its own correlation (Tudose et al. 2009), with a coupling index of $\beta = 0.76 \pm 0.15$ when only the hard states are considered (Tetarenko et al. 2016). The neutron star transient EXO 1745−248 in the globular cluster Terzan 5 traced a $\beta = 1.7 \pm 0.1$ correlation during its 2015 outburst, albeit a factor of five less luminous in the radio band than 4U 1728−34 and Aql X–1 (Tetarenko et al. 2016), suggesting different normalizations for different sources.

The measurement of correlation normalizations, however, can be biased by incorrect distance estimates (Jonker et al. 2004). Deller et al. (2015) suggested that tMSPs may trace a radio–X-ray path of the same slope as black holes, but with a lower normalization, having radio jets that are five times fainter than black holes but one order of magnitude brighter than ordinary neutron stars. They also suggested the relative radio loudness of tMS Ps could be produced by a radiatively inefficient flow, possibly due to the ejection of matter in the propeller regime.

With the exception of the tMSPs, which have radio detections below $L_X \lesssim 10^{36}$ erg s^{-1}, the majority of radio detections in the above studies are of neutron stars in the range $L_X = 10^{36}$–10^{37} erg s^{-1}. This makes the measurement of the correlation index β uncertain due to the short lever arm in X-ray luminosity. X-ray luminosities should be sampled over more than two orders of magnitude to ensure that the measured β does not sample temporary deviations from the underlying correlation (Corbel et al. 2013). Here, we report new and archival radio and X-ray observations of four neutron star X-ray binaries, carried out to track jet behaviour below $L_X = 10^{36}$ erg s^{-1}. Our target sample consists of Cen X−4, it being the closest known quiescent neutron star low-mass X-ray binary (1.2 kpc), and the AMXPs IGR J17511−3057, SAX J1808.4−3658 and IGR J00291+5934, which all underwent outbursts in 2015. With this sample, we can track the radio–X-ray behaviour of ordinary neutron stars and AMXPs and compare them to tMSP and black hole systems.

2 TARGETS

2.1 Quiescent neutron star transient

2.1.1 Cen X−4

Cen X−4, a likely atoll source, was discovered during an outburst in 1969 (Conner, Evans & Belian 1969; Evans, Belian & Conner 1970). During a subsequent outburst in 1979 (Kaluzienski, Holt & Swank 1980), it was also detected in the radio band by the Very Large Array, which was being built at that time (Hjellming 1979; Hjellming et al. 1988). Cen X−4 has been in quiescence ever since, although the currently variable X-ray emission indicates that it is still actively accreting, albeit at a very low level ($L_X = 10^{32}$ erg s^{-1}; Campana et al. 2000, 2004a; Cackett et al. 2010; Bernardini et al. 2013). Given the radio detection of the tMSP PSR J1023+0038 in its accretion state (Deller et al. 2015), during which it has a similar X-ray luminosity as Cen X−4 in quiescence, and indications of a jet in the quiescent AMXP XTE J1814–338 (Baglio et al. 2013), we hypothesize that a jet could still be launched in Cen X−4 even at extremely low X-ray luminosities ($L_X \approx 10^{-6} L_{Edd}$).

Based on the theoretical Eddington luminosity for a neutron star, the Type I X-ray bursts of Cen X−4 place it at a distance of 1.2 ± 0.3 kpc (Chevalier et al. 1989). Using the empirical Eddington luminosity calibrated for neutron stars in globular clusters, González Hernández et al. (2005) report a similar distance of 1.4 ± 0.3 kpc. For consistency with other studies of Cen X−4, we adopt a distance of 1.2 kpc.

As the most nearby known neutron star X-ray binary, Cen X−4 is a good laboratory for testing whether ordinary neutron stars launch jets in quiescence. Previous radio observations of the quiescent Cen X−4, however, have failed to detect a jet, with a 4σ upper limit of $\approx$0.4 mJy (Kulkarni et al. 1992). This upper limit ($L_R < 3 \times 10^{27}$ erg s^{-1}) is unconstraining compared to black holes at the same X-ray luminosity ($L_R \approx 10^{27}$ erg s^{-1}).

2.2 AMXPs in outburst

2.2.1 IGR J17511−3057

Discovered in 2009 by *INTEGRAL* (Baldovin et al. 2009), IGR J17511−3057 was later classified as an AMXP after the detection of 245 Hz X-ray pulsations (Markwardt et al. 2009). Since its 2009 outburst, it has undergone two additional outbursts, in 2012 and 2015. Previous radio observations were conducted by Miller-Jones, Russell & Migliari (2009) during the 2009 September outburst, but no emission was detected, with 3σ upper limits of 0.17 mJy.

Based on the peak X-ray flux of its thermonuclear bursts, Altamirano et al. (2010) placed an upper limit of 6.9 kpc on its distance. Papitto et al. (2010) found a similar lower limit of 6.5 kpc by assuming that the emission during the outburst decay comes from the neutron star surface. The pulsation timing analysis of Riggio et al. (2011) pointed towards two possible distances (6.3 or 3.6 kpc), the first of which is comparable with previous estimates. We adopt a distance of 6.9 kpc for IGR J17511−3057 for consistency with previous studies.

2.2.2 SAX J1808.4−3658

The first detected and most extensively studied AMXP, SAX J1808.4−3658 was discovered in 1996 with the *BeppoSAX* satellite (in 't Zand et al. 1998), and classified as an AMXP after the discovery of a 401 Hz spin (Wijnands & van der Klis 1998). It was previously detected in the radio band during three of its outbursts, in 1998, 2002 and 2005 (Gaensler, Stappers & Getts 1999; Rupen et al. 2002; Rupen, Dhawan & Mioduszewski 2005).

Based on the fluence and recurrence times of its outbursts, Galloway & Cumming (2006) estimated a distance to SAX J1808.4−3658 of 3.4–3.6 kpc, which is consistent with the distance derived from Type I X-ray bursts (3.1–3.8 kpc). We adopt a distance of 3.5 kpc for SAX J1808.4−3658.

The X-ray light curves of SAX J1808.4−3658 are similar between different outbursts. After a quick rise to the outburst peak, the source slowly decays for 15–20 d, followed by a faster decay over $\approx$ 3 d, after which the source reflares for a few tens of days, each reflare lasting a few days (Patruno et al. 2016). Episodic accretion of matter in the propeller regime could be the mechanism behind the reflares (Patruno et al. 2016). At $L_X \approx 10^{33}$ erg s^{-1}, the magnetosphere reaches the light cylinder of the neutron star, so that in quiescence SAX J1808.4−3658 should turn on as a radio pulsar (Campana et al. 2002). However, no radio pulsations have been detected so far (Burgay et al. 2003; Iacolino et al. 2010; Patruno et al. 2017) in quiescence (quiescent $L_X \approx 10^{31}$ erg s^{-1}; Campana et al. 2002), when a typical radio pulsar should have been detected, although the presence of a radio pulsar has been indirectly inferred (Burderi et al. 2003; Campana et al. 2004b).

2.2.3 IGR J00291+5934

Following the discovery of IGR J00291+5934 in 2004 by *INTEGRAL* (Eckert et al. 2004), the detection of a 599 Hz spin frequency by *RXTE* classified it as an AMXP (Galloway et al. 2005). Similar to SAX J1808.4−3658, IGR J00291+5934 goes into outburst every 3–4 yr. During its discovery outburst, the source was also detected in the radio band (Fender et al. 2004b; Pooley 2004; Rupen, Dhawan & Mioduszewski 2004), but no radio emission was detected during its two fainter outbursts in 2008 (Linares, Tudose & Migliari 2008;

Lewis et al. 2010). Similar to SAX J1808.4−3658, there is some evidence that IGR J00291+5934 might become active as a radio pulsar during quiescence (Jonker, Torres & Steeghs 2008).

A Type I X-ray burst from IGR J00291+5934 was detected for the first time during the 2015 outburst, placing it at a distance of 4.2 ± 0.3 kpc (Bozzo et al. 2015b; De Falco et al. 2017). This measurement is in line with the lower limit of ≈ 4 kpc based on the fluence of the 2004 outburst (Galloway et al. 2005). However, Jonker et al. (2005) and Torres et al. (2008) found that IGR J00291+5934 should lie 2–3.6 kpc away, assuming a similar quiescent X-ray flux as other AMXPs. Torres et al. (2008) also estimated a lower limit of 1.8–3.8 kpc based on the timing of the fast decay in its X-ray light curve, and assumptions on disc ionization states. In this work, we assume a distance of 4.2 kpc to IGR J00291+5934, since it is based on Type I X-ray bursts.

3 OBSERVATIONS

3.1 Cen X−4

On 2015 January 17, we observed Cen X−4 in quiescence simultaneously with the Karl G. Janksy Very Large Array (VLA), proposal code 14B-117) and the *Swift* X-ray Telescope (XRT; Gehrels et al. 2004; Burrows et al. 2005), under a Target of Opportunity observation (ObsID 00035324066). The VLA observations were carried out when the array was in the CnB configuration, at 8–12 GHz, between 13:06 and 13:48 UT, with an on-source integration time of 34 min. The XRT observations started at 13:25 UT, for a deadtime-corrected exposure time of 936 s in photon counting (PC) mode.

3.2 IGR J17511−3057

An outburst from IGR J17511−3057 was detected by *INTEGRAL* on 2015 March 23 (Bozzo et al. 2015a; Papitto et al. 2016). We observed this source with the VLA (proposal code 14B-153) on three occasions over 2 weeks, during a period of X-ray monitoring with *Swift*/XRT (detailed in Papitto et al. 2016). Our radio observations were carried out when the VLA was in B configuration, at 8–12 GHz. Because IGR J17511−3057 remained undetected in all these observations, we then switched to observing SAX J1808.4−3658, which went into outburst during our monitoring campaign on IGR J17511−3057.

3.3 SAX J1808.4−3658

The *Swift*/BAT monitor detected a new outburst from SAX J1808.4−3658 on 2015 April 9 (Sanna et al. 2015), which we subsequently monitored with the VLA (proposal code 14B-153) in B configuration, during the decay phase in April and May. On April 19, we observed this source simultaneously in the *C* (4–8 GHz) and *K* (18–26.5 GHz) bands, for improved spectral information at peak luminosity. The high-frequency *K*-band observations required pointing calibration, for which we observed the bright calibrator J1820−2528. All the other observations were taken in the *X* (8–12 GHz) band. The outburst was monitored in X-rays with *Swift*/XRT with almost daily cadence (the observation log is given in Table 1). For comparison with the X-ray and radio data, we also report optical observations (Bernardini et al., in preparation).

We monitored the 2015 outburst of SAX J1808.4−3658 at optical wavelengths with the 2-m robotic Faulkes Telescopes North

Table 1. *Swift*/XRT observations of SAX J1808.4−3658 in window timing (WT) and PC modes.

Programme IDs	Obs. number	Obs. mode	Date	Exposure (s)
30034	74	WT	2015-04-13	5184
	76	WT	2015-04-14	1618
	77	WT	2015-04-15	839
81453	01	WT	2015-04-16	1794
33737	01	WT	2015-04-17	5179
30034	78	WT	2015-04-18	1848
	79	WT	2015-04-19	389
	80	WT	2015-04-20	621
	81	WT	2015-04-21	1969
	82	WT	2015-04-22	2188
33737	02	PC	2015-04-24	3719
	03	PC	2015-04-29	2544
	04	PC	2015-04-30	5444
33034	83	PC	2015-05-02	418
	84	PC	2015-05-03	1118
	85	PC	2015-05-04	1003
	86	PC	2015-05-05	684
	87	PC	2015-05-06	1118
33737	05	PC	2015-05-09	5855
30034	88	PC	2015-05-09	975
	90	PC	2015-05-10	1041
	89	PC	2015-05-10	1076
	91	PC	2015-05-12	1166
	92	PC	2015-05-13	968
33737	06	PC	2015-05-15	3707
30034	94	PC	2015-05-19	995

and South, located at Haleakala on Maui and Siding Spring, Australia, respectively, as part of an ongoing monitoring campaign of ∼40 low-mass X-ray binaries (Lewis et al. 2008). During the outburst, we increased the cadence and made additional observations with five of the robotic 1-m telescopes in the Las Cumbres Observatory (LCO) network; namely one located at the Cerro Tololo Inter-American Observatory, Chile, two at the South African Astronomical Observatory, Sutherland, South Africa, and two at Siding Spring Observatory, Australia. Photometric observations were made using four filters; Bessell *B* band, *V* band, *R* band and Sloan Digital Sky Survey *i'* band. Here, we present the data in *i'* band only, which have the most number of observations during the outburst, and are sufficient to characterize the optical light curve, identify flares, and compare to the X-ray and radio light curves.

3.4 IGR J00291+5934

Following the optical discovery of a new outburst from IGR J00291+5934 on 2015 July 24 by *Swift*/BAT (Cummings et al. 2015), in August we carried out three radio observations with the VLA in A configuration, at 8–12 GHz, under Director's Discretionary Time (proposal code 15B-339).

3.5 Data analysis

3.5.1 VLA

The radio observations of all four systems are summarized in Table 2. We calibrated the radio data from the VLA with the Common Astronomy Software Applications package (CASA v4.2.1; McMullin et al. 2007) using standard procedures. The source 3C48 was used as a flux calibrator for IGR J00291+5934, and 3C286 for the other sources. For all four sources, we switched between

Table 2. Summary of VLA radio observations.

Source	Project ID	Date (2015)	Integration time (min)	Array configuration	Observing band (GHz)	Phase calibrator
Cen X−4	14B-117	17 January	34	CnB	X (8.0–12.0)	J1522−2730
IGR J17511−3057	14B-153	26 March	13	B	X	J1744−3116
		2 April	13		X	
		8 April	12		X	
SAX J1808.4−3658	14B-153	18 April	11	B	X	J1744–3116
		19 April	11		K (18.0–26.5)	
		19 April	15		C (4.0–8.0)	
		22 April	11		X	
		27 April	12		X	
		5 May	11		X	
		7 May	22		X	
		10 May	23		X	
IGR J00291+5934	15B-339	11 August	36	A	X	J0102+5824
		15 August	36		X	
		18 August	36		X	

Table 3. Radio monitoring results. Source distances are assumed as discussed in Section 2.

Source	D (kpc)	MJD	$F^a_{1-10\,\mathrm{keV}}$ ($\times 10^{-11}$ erg cm^{-2} s^{-1})	ν (GHz)	S_ν (μJy bm^{-1})	α
Cen X−4	1.2	56650.409	$(8.5 \pm 5.4) \times 10^{-3}$	10.0	<14	–
IGR J17511−3057	6.9	57107.592	58.5 ± 10.1	10.0	<22	–
		57114.432	38.9 ± 6.7	10.0	<21	–
		57120.494	27.0 ± 4.6	10.0	<28	–
SAX J1808.4−3658	3.5	57130.411	98.7 ± 5.5	10.0	317 ± 24	0.05 ± 0.45
		57131.413	91.4 ± 5.1	22.0	238 ± 23	– [b]
		57131.427	91.4 ± 5.1	6.0	321 ± 25	-0.24 ± 0.10[b]
		57134.397	73.0 ± 4.1	10.0	277 ± 22	-0.51 ± 0.56
		57139.386	50.0 ± 2.8	10.0	426 ± 24	-0.21 ± 0.60
		57147.415	1.6 ± 0.1	10.0	63 ± 13	– [c]
		57149.484	1.9 ± 0.1	10.0	174 ± 9	-0.26 ± 0.57
		57152.478	11.1 ± 0.6	10.0	50 ± 8	– [c]
IGR J00291+5934	4.2	57245.376	19.6 ± 7.2	10.0	46 ± 8	– [c]
		57249.335	0.65 ± 0.16	10.0	15 ± 7	– [c]
		57252.241	$(3.6 \pm 2.8) \times 10^{-2}$	10.0	<12	–

Notes. [a]Estimated at the time of the radio observation.
[b]The 6 and 22 GHz observations were used to derive a single spectral index measurement.
[c]The signal-to-noise ratio is too low for a meaningful spectral index measurement.

phase calibrator and science target on 5 min cycles (3 min for the 22 GHz observations). We imaged the Stokes I data using Briggs weighting with a robustness parameter of 1 as a compromise between sidelobe contamination and point-source sensitivity. We performed deconvolution using the multifrequency, multiscale `clean` algorithm with two Taylor coefficients to account for sky frequency dependence. No self-calibration was performed. The flux density of each detected source was measured by fitting the source in the image plane using the `imfit` task. We forced a point-source fit, with an elliptical Gaussian of the shape of the synthesized beam. The flux uncertainty is taken as the rms of the residual image, with an additional systematic uncertainty of 2 per cent, typical of flux calibration with the VLA at these frequencies. Given that no self-calibration was performed, the flux errors could be underestimated. The observing frequencies (primarily centred at 10 GHz), and the short phase-referencing cycle times (5 min), should help to minimize the effects of phase decorrelation. While the lack of other point sources in the fields of view of our targets means we cannot quantify the level of phase decorrelation, we assume it to be negligible for the reasons stated above. Our

final flux density measurements are given in Table 3. The flux density upper limits on non-detections are reported at three times the local rms.

To measure the radio spectral index of SAX J1808.4−3658, we split each 10 GHz observation into two sub-bands (8–10 and 10–12 GHz) and imaged them separately. On April 19, we carried out 6 and 22 GHz observations for a more precise measurement of the spectral index. We use the flux densities measured at each of these two frequencies to obtain the spectral index α following the $S_\nu \propto \nu^\alpha$ convention (where S_ν is the flux density measured at the central frequency ν).

We also calibrated previously unpublished Very Large Array observations of IGR J00291+5934 taken during the 2004 (proposal code AR545 on December 11 and 14, taken in A configuration at 4.86 GHz) and 2008 (proposal code MPRTST on September 30 in D configuration at 8.46 GHz) outbursts. As in our 2015 observations, the phase calibrator was J0102+5824 for all these observations, and the flux calibrator was 3C286 in 2004 and 3C147 in 2008. For these archival observations, we used only one Taylor coefficient during deconvolution (suitable for these single-frequency

observations) and natural weighting (to maximize point-source sensitivity).

3.5.2 Swift

Swift/XRT data were analysed with HEASOFT, as part of the HEASARC software suite (Arnaud 1996). To generate the *Swift*/BAT light curves, we used the *Swift*/BAT light-curve data base (Krimm et al. 2013).

During our single X-ray observation of Cen X−4 on 2015 January 17 (MJD 56650.4), *Swift*/XRT operated in PC mode (2.5 s resolution). Within a 20 arcsec radius of its position, only seven total counts are detected (corresponding to a count rate of 7.5×10^{-3} counts s^{-1}). The background level was measured in an area offset from visible X-ray sources. Given the low number of counts, we do not fit its spectrum, but assume the same spectral shape as that reported by Bernardini et al. (2013) for the faintest state of Cen X−4 (count rate <0.07 counts s^{-1}), and use Poisson statistics (Kraft, Burrows & Nousek 1991) to estimate the 90 per cent confidence interval for its count rate. We assume a low-luminosity spectrum for Cen X−4 consisting of a thermal component (which dominates at energies below ≈ 2 keV) and a power-law component ($\Gamma = 2.0$), absorbed by a column density $N_{\mathrm{H}} = 8 \times 10^{20}$ cm^{-2} (Bernardini et al. 2013). When calculating the uncertainty in the count rate, we only take into consideration the errors associated with the low number of counts, since they will dominate over the errors associated with the spectral model. We use XSPEC (12.9.0) and WebPIMMS[1] (Mukai 1993) to convert from count rate to un-absorbed flux.

For IGR J17511−3057, we use the light curve and spectral information provided by Papitto et al. (2016), observed with *Swift*/XRT in WT (1.76 ms resolution) and PC modes. They fit the spectra with an absorbed power law, and reported the fluxes in the 0.5–10 keV range (for the same 6.9 kpc distance assumed in this work), which we converted to 1–10 keV fluxes in WebPIMMS, using their measured absorption column and photon indices.

For SAX J1808.4−3658, we analysed all pointed *Swift*/XRT observations taken between 2015 April 13 (MJD 57125.4) and 2015 May 19 (MJD 57161.8). A total of 26 observations were taken, with Programme IDs 33034, 33737 and 81453. The X-Ray Telescope operated either in WT or in PC mode. The source counts were extracted in an energy range of 1–10 keV, as is commonly used in recent literature, from a circular region of radius 20 arcsec, and the background was extracted from an area far from known sources in the field. The events and X-ray spectra were extracted with the tool XSELECT (v2.4d) and the spectral analysis was done with XSPEC. Each spectrum was fitted with a simple absorbed power-law model plus a multiplicative component (CFLUX) used to calculate the unabsorbed flux in the 1–10 keV band (and its 90 per cent confidence interval).

For IGR J00291+5937, we use a procedure similar to that described for SAX J1808.4−3658. The observation campaign carried out with *Swift*/XRT on this source will be described in full in Russell et al. (in preparation).

3.5.3 Ariel V

For the 1979 outburst of Cen X−4, we use the X-ray data reported by Kaluzienski et al. (1980), observed with the Ariel V All-Sky X-ray Monitor (Holt 1976), and retrieved from the public archive.

---

[1] https://heasarc.gsfc.nasa.gov/docs/software/tools/pimms.html

We converted the reported 3–6 keV flux to 1–10 keV unabsorbed flux using WebPIMMS, by assuming a power-law spectrum with photon index $\Gamma = 1.6$ (as adopted by Bernardini et al. 2016) and absorption $N_{\mathrm{H}} = 8 \times 10^{20}$ cm^{-2} (Bernardini et al. 2013).

3.5.4 RXTE

To estimate the X-ray fluxes of IGR J00291+5934 at those times when the source was not detected in the radio band during its outbursts in 2004 and 2008, we used the X-ray data reported by Galloway et al. (2005) and Lewis et al. (2010), observed with the *RXTE* Proportional Counter Array. These data were retrieved from the XTE Mission-Long Source Catalog. We converted the 2–9 keV count rate from IGR J00291+5934 to the 1–10 keV unabsorbed flux using WebPIMMS, by assuming a power-law spectrum with photon index $\Gamma = 2.06$ and absorption $N_{\mathrm{H}} = 4.3 \times 10^{21}$ cm^{-2}, which describes the 0.4–10 keV spectrum (Paizis et al. 2005).

3.5.5 LCO

The i'-band magnitudes were extracted using PHOT in IRAF and calibrated using the three comparison stars listed in Greenhill, Giles & Coutures (2006). i'-band magnitudes of the three comparison stars were calculated from R- and I-band magnitudes using the conversion of Jordi, Grebel & Ammon (2006), in the same way as mentioned in Elebert et al. (2009).

4 RESULTS

4.1 Cen X−4

We did not detect Cen X−4 in the radio band, although we place constraints on the emission (<14 μJy; Table 2) that are a factor of ≈ 20 deeper than previous radio observations in quiescence (Kulkarni et al. 1992). In the X-ray band, we detected only seven total photons (including background) from Cen X−4, as our observations were conducted during a particularly faint X-ray state (Fig. 1). The 90 per cent confidence interval for its background-subtracted 1–10 keV luminosity is $L_{\mathrm{X}} = 8.0 \times 10^{30}$ to 5.6×10^{31} erg s^{-1}.

4.2 IGR J17511−3057

We conducted radio observations of IGR J17511−3057 during its slow X-ray decay (Fig. 2). Similar to previous outbursts, it remained undetected in the radio band, although our constraints (<21 μJy; Table 2) are a factor of ≈ 8 deeper than previous radio observations at similar X-ray luminosity (Miller-Jones et al. 2009).

4.3 IGR J00291+5934

Our radio observations were conducted during the fast X-ray decay of IGR J00291+5934 (Fig. 3), and we detected it in the first two of three epochs (Table 2). We did not detect the source in the archival observations taken on December 11 (<132 μJy) and 14 (<111 μJy), 2004 or on 2008 September 30 (<156 μJy). Coupled with previous detections, IGR J00291+5934 now has a well-sampled X-ray luminosity range, meaning that we can track its disc–jet coupling from the peak of the outburst towards quiescence (Fig. 5), assuming that it follows the same path over multiple outbursts, as seen in the black holes GX 339−4 (Corbel et al. 2013) and V404 Cyg (Plotkin et al. 2017).
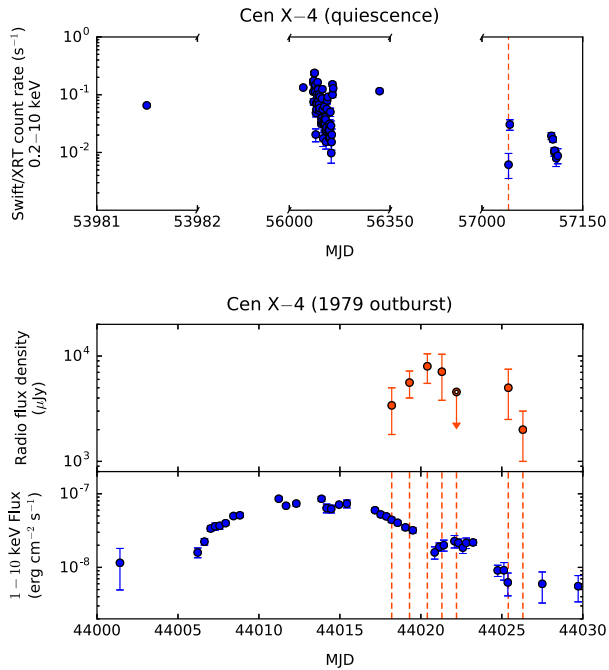
Figure 1. *Top*: Quiescent X-ray light curve of Cen X−4, as observed by *Swift*/XRT in PC mode. We show all observations with the *Swift*/XRT (over the years 2006/2012/2015) as a visual representation of the quiescent flux of Cen X−4. The blue points show individual snapshots and the vertical dashed line indicates the timing of our VLA observations in 2015, carried out simultaneously with an XRT observation when the system was in a particularly faint state. *Bottom*: The radio and X-ray light curves of Cen X−4 during its 1979 outburst, as observed with the VLA (Hjellming et al. 1988) and the Ariel V satellite (Kaluzienski et al. 1980). Cen X−4 was detected in the radio band multiple times during the X-ray decay.
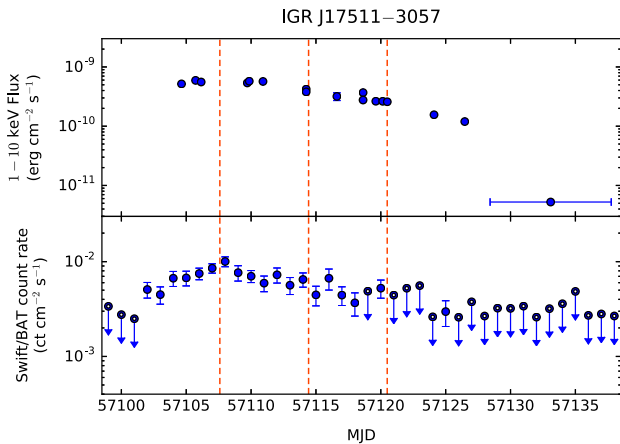
Figure 2. X-ray light curves of IGR J17511−3057 during its outburst in 2015, as observed by *Swift*/XRT (1–10 keV flux) and *Swift*/BAT (15–150 keV count rate). The blue points show individual observations and the vertical dashed lines indicate the timing of our VLA observations. All radio observations were carried out during the slow X-ray decay. We did not detect the source in any of our VLA observations.

4.4 SAX J1808.4−3658

4.4.1 Light curves

The seven radio detections of SAX J1808.4−3658 (labelled sequentially A–G) at different times across a single outburst make
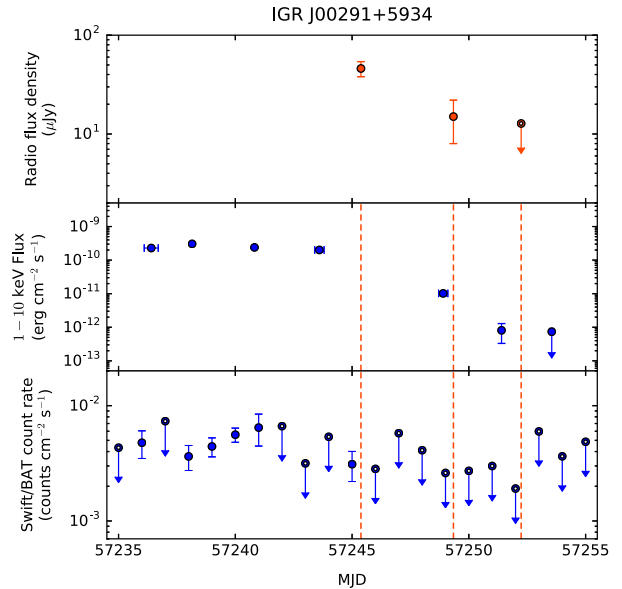
Figure 3. The radio (VLA) and X-ray (*Swift*/XRT, 1–10 keV flux; *Swift*/BAT, 15–150 keV count rate) light curves of IGR J00291+5934 during the late stages of its 2015 outburst. We detect the source in the first two out of our three observations.
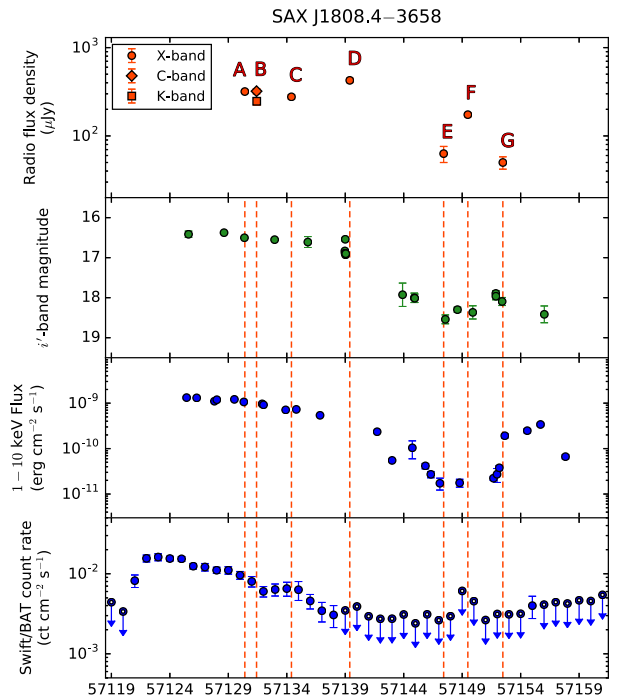

Figure 4. Radio (VLA), optical (LCO) and X-ray (*Swift*/XRT, 1–10 keV flux; *Swift*/BAT, 15–150 keV count rate) light curves of J1808.4−3658 during its 2015 outburst. The orange dashed lines indicate the times of the radio observations, individually labelled from A to G. During the slow X-ray decay, the source undergoes a radio reflare (observation F).

it an excellent source for tracing the inflow–outflow coupling in an AMXP. Observations during previous outbursts have identified SAX J1808.4−3658 as a radio-loud neutron star (Migliari & Fender 2006), and in addition to the main outburst, we are now also able to track its multiwavelength behaviour in the fainter states (Fig. 4).

In X-rays, SAX J1808.4−3658 behaved during its 2015 outburst similarly to previous outbursts: a slow decay (until MJD ≈57141), a fast decay (MJD ≈ 57141 − 57143) and a reflaring tail (after MJD ≈ 57143). A radio reflare was also observed, but the X-ray and radio reflares do not seem to be coincident (observations F, G in Fig. 4). Radio detections during X-ray reflares show that the jet survives during the reflaring tail. The last two radio observations show unexpected behaviour, as the source undergoes a radio reflare during an X-ray minimum (observation F, although an X-ray reflare at that time could have been missed, see Section 5.3.1), and no increase in radio flux is observed during a rapid increase in X-ray flux at the start of an X-ray reflare (observation G). We find little evidence of intra-observation variability during these two radio observations (consistent with a constant flux over 2 and 10 min time-scales within ≈2σ uncertainty).

4.4.2 Radio spectral indices

The 6 and 22 GHz observations from April 19 were taken within 20 min of each other, during which time we do not expect the source to have varied (see Section 4.4.1). Indeed, we do not find evidence for variability during either observation on that day (both C- and K-band data are consistent with a constant flux within each observation within 1σ uncertainty). We find the spectral index to be close to flat ($\alpha = -0.24 \pm 0.10$, assuming no change in flux between the two observations), similar to the compact jets of other X-ray binaries, although we cannot rule out a steep spectrum within uncertainties. We find that the spectral index measurements within the 10 GHz band on the other observing epochs are typically unconstraining (with a typical error of ±0.5, due to the faintness of the radio emission and the small lever arm in frequency), so we cannot distinguish between optically thin and thick emission. The spectral index measurements for all epochs are listed in Table 3.

4.5 The radio–X-ray correlation

The radio ($L_R = 4\pi D^2 \nu S_\nu$, where D is the distance to the source) and X-ray luminosities of our sample are displayed in Fig. 5 individually, and together in Fig. 6, with the addition of other black hole and neutron star systems from the literature.

Positions of X-ray binaries on the radio–X-ray plane are best measured from strictly simultaneous observations. Among our multiwavelength campaign, Cen X−4 has strictly simultaneous data. For the other sources, we interpolate the X-ray light curve to estimate the X-ray flux at the time of the radio observations, by fitting a piecewise linear function in the log L_X/time space.

The 3 σ upper limit of 14 μJy on the radio emission of Cen X−4 in quiescence only constrains its radio luminosity to being less than that of the radio-fainter black hole jets (e.g. XTE J1118+480; Gallo et al. 2014). The limit lies just above the proposed tMSP track, slightly below the quiescent black hole systems.

In addition, we also place the 1979 outburst of Cen X−4 on the radio/X-ray plane for the first time. For the radio luminosity, we use the data reported by Hjellming et al. (1988) in two bands (at 1.49 and 4.9 GHz). For days when observations were carried out in both radio bands, we use the measurement with smaller uncertainties, with the assumption of a flat spectrum. We find that during the 1979 outburst, Cen X−4 reached radio and X-ray luminosities similar to the atoll sources. Assuming it follows a single, continuous radio–X-ray correlation from the peak of the outburst down to quiescence (like the black hole systems V404 Cyg, Corbel et al. 2008; and
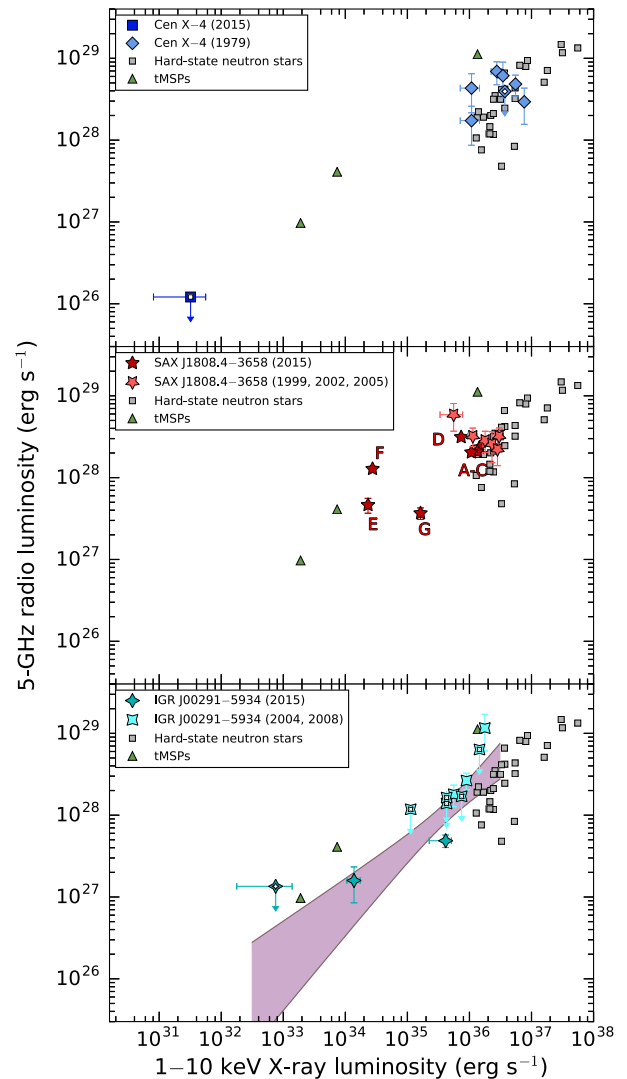

Figure 5. The radio and X-ray luminosities of Cen X−4, SAX J1808.4−3658 and IGR J00291+5934. Hollow symbols mark upper limits. The labelled data points of SAX J1808.4−3658 refer to the same observations in Fig. 4. IGR J00291+5934 (and possibly SAX J1808.4−3658, but with larger scatter) seems to follow the familiar $L_R \propto L_X^\beta$ correlation seen in black holes and some atoll sources, with $\beta = 0.77 \pm 0.18$ (90 per cent confidence interval, shaded area).

GX 339–4, Corbel et al. 2013), we obtain a lower limit for its correlation slope $\beta \gtrsim 0.5$.

The upper limits for IGR J17511–3057 make it less luminous in the radio band than typical atoll sources (Fig. 6), but we cannot rule out radio emission at a level similar to that of EXO 1745−248, the radio-detected neutron star with the lowest disc–jet coupling normalization (Tetarenko et al. 2016).

Previous radio detections of SAX J1808.4−3658 sample just one decade of X-ray luminosity ($L_X \approx 10^{35}$ to 10^{36} erg s^{-1}; Migliari, Miller-Jones & Russell 2011). Here, we extend the range of detections down to $L_X \approx 10^{34}$ erg s^{-1}. The radio behaviour of SAX J1808.4−3658 during the slow X-ray decay seems to be reproducible between different outbursts, with a clustering of detections at $L_X \approx 10^{36}$ erg s^{-1} and $L_R \approx 10^{28}$ erg s^{-1}. As it fades, SAX J1808.4−3658 is seen to alternate between the atoll sources and tMSPs in the radio–X-ray plane. This points to
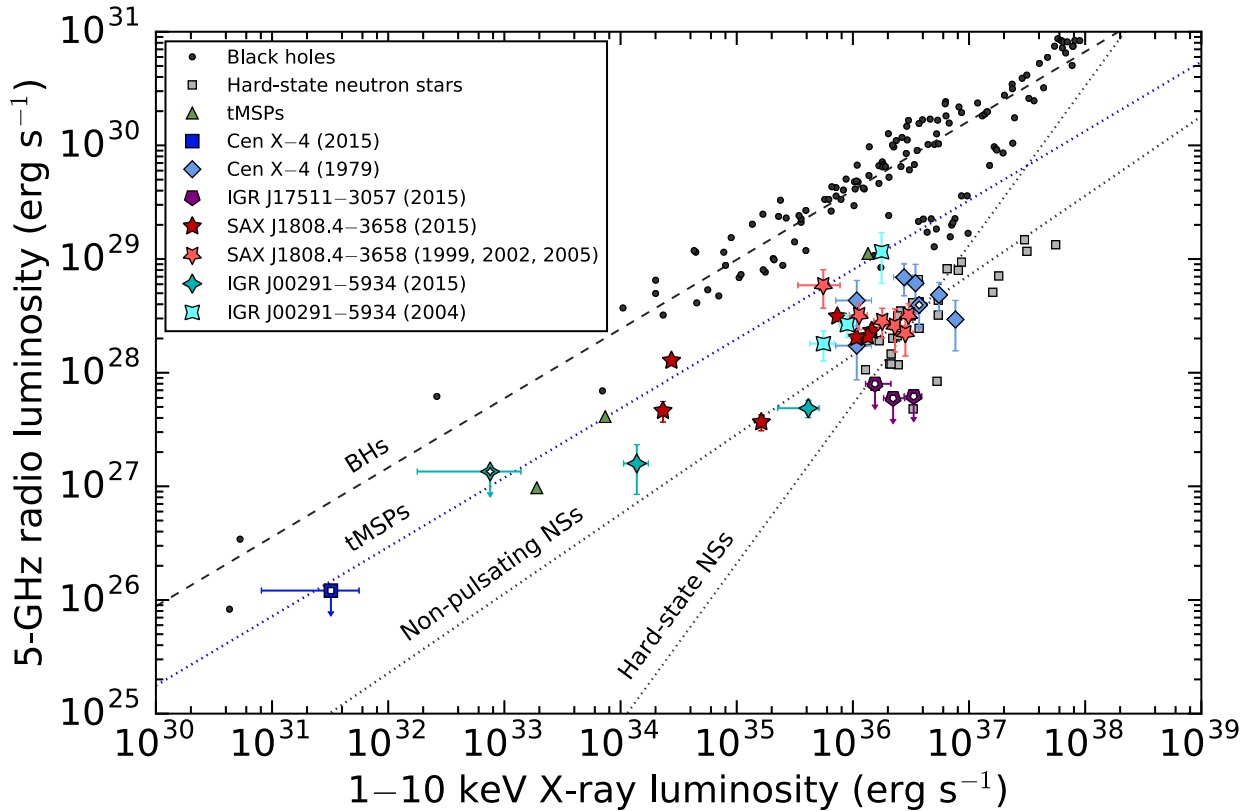
Figure 6. Radio and X-ray luminosities of low-mass X-ray binaries. The black dashed line represents the radio–X-ray correlation of accreting black holes ($\beta = 0.6$; Gallo et al. 2014), and the three dotted lines are the proposed relations for tMSPs ($\beta = 0.6$; Deller et al. 2015), non-pulsating neutron stars regardless of spectral state ($\beta = 0.7$) and hard-state neutron stars only ($\beta = 1.4$; Migliari & Fender 2006; Migliari et al. 2011). Hollow symbols indicate upper limits. The upper limits from the previous outbursts of IGR J00291+5934 are not plotted for better visibility.

temporal changes in the radiative efficiency, which does not reach the same levels as for black hole systems.

Similar to SAX J1808.4−3658, our radio observations of IGR J00291+5934 make it possible to study the jet over two decades of X-ray luminosity, in the range $L_X \approx 10^{34}$–10^{36} erg s^{-1}. In contrast to SAX J1808.4−3658, IGR J00291+5934 is consistent with following a $L_R \propto L_X^\beta$ correlation. We find a correlation slope $\beta = 0.77 \pm 0.18$ (90 per cent uncertainty range, assuming reproducible outbursts), which is similar to the primary black hole track, to the proposed tMSP track, and to Aql X−1 (above 10^{36} erg s^{-1}; Tetarenko et al. 2016), at a luminosity similar to that of atoll sources.

5 DISCUSSION

Our results reinforce the idea of different behaviours in different neutron star systems – with reflares and no consistent radio–X-ray relationship (SAX J1808.4−3658), with a well-fitting radiatively inefficient flow (IGR J00291+5934), long-term steady, but with flipping between X-ray modes (tMSPs), etc. Our observations strengthen the evidence for atoll sources and AMXPs being fainter in the radio band than black holes at the same X-ray luminosity. Some AMXPs can be faint (IGR J00291+5934) or fainter than non-pulsating neutron stars (IGR J17511−3057). During outbursts, however, some AMXPs (SAX J1808.4−3658) can become as radio-bright as tMSPs (a conclusion also supported by the tMSP M28I, which was observed in outburst as an AMXP; Papitto et al. 2013).

The above hints at a maximum radio luminosity achievable by neutron stars, a factor of ≈5 fainter than radiatively inefficient black holes at the same X-ray luminosity, as proposed by Deller et al. (2015). One expects radio jets from more massive accretors to be more luminous, as indicated by the Fundamental Plane of accreting black holes ($\log L_R \propto 0.8 \log M$; Merloni, Heinz & di Matteo 2003; Falcke, Körding & Markoff 2004). Therefore, as already noted by Deller et al. (2015), the difference in mass between black holes ($\approx 8\,M_\odot$; Özel et al. 2010; Kreidberg et al. 2012) and neutron stars ($\approx 1.4\,M_\odot$; Özel et al. 2012) could account for a factor of ≈4 between the radio luminosity of the two classes of X-ray binaries, if their accretion mechanisms are otherwise similar. This could possibly explain some of the difference between the radiatively inefficient black holes, and the most radio-luminous neutron stars (the tMSPs, and the radio-loud epochs of SAX J1808.4−3658).

Because of different disc–jet coupling behaviours in different neutron stars, highlighted by the contrast between IGR J00291−3658, with a coupling index $\beta \approx 0.7$, and EXO 1745−248, with $\beta \approx 1.7$ (Tetarenko et al. 2016), we do not attempt to fit a single radio/X-ray correlation for the whole population of neutron stars (as previously done by Migliari & Fender 2006). Such a fit would be biased towards radio-loud neutron stars, and would thus offer neither further insights into the accretion process, nor better predictive power. As a tool to identify new black holes and neutron star candidates below $L_X \lesssim 10^{36}$ erg s^{-1}, we therefore advise only using the maximal radio luminosity (neutron stars at least a factor of ≈5 fainter than black holes) suggested above.

Below we discuss each source in our sample, considering in most detail the case of SAX J1808.4−3658, the source for which we obtained the best-sampled multiwavelength coverage.

5.1 Cen X−4

The X-ray flux of Cen X−4 during our observations was an order of magnitude lower than its median quiescent flux (see Fig. 1). Its quiescent X-ray luminosity (Cackett et al. 2010; Bernardini et al. 2013) is typically in the range $L_X = 0.7$–4.3×10^{32} erg s^{-1} in the 1–10 keV band (assuming a photon index $\Gamma = 1.5$). In contrast, we measure a luminosity $L_X \approx 0.05$–0.24×10^{32} erg s^{-1} (90 per cent uncertainty range), which means that we cannot place constraints on jet production in Cen X−4 in quiescence, deeper than that of some black holes.

During its outburst in 1979, Cen X−4 had similar radio ($L_R = 10^{28}$–10^{29} erg s^{-1}) and X-ray luminosities ($L_X = 10^{36}$–10^{37} erg s^{-1}) as most of the non-pulsating systems. The signal-to-noise ratio of these early radio detections, however, is too low to check if the two wavebands are correlated. Including our radio upper limit during quiescence, the radio–X-ray correlation index is only restricted to $\beta \gtrsim 0.5$, so we cannot differentiate between radiatively efficient or inefficient accretion in this system.

Had we observed Cen X−4 at a more typical quiescent X-ray luminosity, a radio observation would have likely either detected or disproved the formation of a jet as powerful as that of tMSPs. We therefore encourage future simultaneous radio and X-ray observations of Cen X−4.

5.2 IGR J17511−3057

The radio non-detection of IGR J17511−3057 could potentially be attributed to several factors: an incorrect distance estimate, a quenching of the jet in the soft state or suppression of jet formation by a high magnetic field. IGR J17511−3057 would need to be located approximately 30 kpc away for its upper limits to be consistent with the $\beta = 0.7$ correlation for neutron stars. Given that multiple distance estimates point towards a source distance of less than 7 kpc (see Section 2.2.1), we consider that its non-detection has a physical origin. Jet quenching at high Eddington ratios has previously been observed in the atoll sources Aql X-1 (Tudose et al. 2009; Miller-Jones et al. 2010), GX 9+9 (Migliari 2011) and 4U 1728–34 (Migliari et al. 2003), but it has not been seen in all neutron stars (Rutledge et al. 1998; Migliari et al. 2004). The hard spectral state and power spectrum of the low-luminosity outburst of IGR J17511−3057 (Papitto et al. 2016) point towards a canonical hard state (Shaposhnikov & Titarchuk 2006) and hence, against the non-detections being caused by jet quenching in the soft state.

The high magnetic fields of pulsars may also inhibit the formation of jets (for fields $\gtrsim 10^{11}$ G; Fender & Hendry 2000; Migliari et al. 2012), although the magnetic field of IGR J17511−3057 has been estimated to be similar to that of other AMXPs ($\sim 10^8$ G; Mukherjee et al. 2015; Papitto et al. 2016). The detection of type I bursts (Altamirano et al. 2010) also rules out a high magnetic field (Joss & Li 1980).

Given that radio emission at the same level as EXO 1745−248 is not ruled out, it is possible that IGR J17511−3057 has an X-ray to radio normalization that is lower than that of other AMXPs and atolls. Contrary to the common assumption that AMXPs are more radio-loud than non-pulsating sources, IGR J17511−3057 would then be a clear example that this rule does not hold for all AMXPs. Since IGR J17511−3057 has a similar spin ($\nu = 245$ Hz) and magnetic field strength ($B \approx 10^8$ G) to other AMXPs (Mukherjee et al. 2015), it appears that the magnitude of the spin and magnetic field are not the only properties that produce strong jets in the other

AMXPs and tMSPs, and that other factors, as yet unidentified, could be at least as important.

5.3 SAX J1808.4−3658

The atypical radio behaviour of SAX J1808.4−3658 might be interpreted in a variety of ways, which we explore below. Throughout this section, we refer to our radio epochs as A–G, as labelled in Fig. 4. Of these, we refer to those epochs that are close to the proposed radio/X-ray correlation for tMSPs as 'radio-loud' (our observations D, E, F, and the detection by Gaensler et al. 1999).

5.3.1 Insufficient light-curve sampling

Sparse X-ray coverage could be invoked to explain the apparent high radio luminosity of the radio-loud epochs, and their deviation from the proposed radio/X-ray tracks for neutron stars. For example, *Swift*/XRT observations might have missed an X-ray reflare coincident with the radio reflare of observation F. The X-ray reflares can last as little as ≈0.3 d (Wijnands et al. 2001). In comparison, the two *Swift*/XRT observations adjacent to the radio reflare (observation F) are separated by ≈3 d. We therefore examine hard X-ray (*Swift*/BAT, 15–50 keV) and optical (LCO) light curves for evidence of flares or dips of other wavebands at the times of the radio observations. We find the optical and soft X-ray fluxes in SAX J1808.4−3658 track each other well during the outburst (Fig. 4; a full description of the optical–X-ray correlation will be presented in Bernardini et al.), similar to previous outbursts (Patruno et al. 2016). In previous outbursts, however, the X-ray lagged the optical emission by 1.5–4 d (Giles et al. 1999; Patruno et al. 2016), and the optical and X-ray fluxes during some reflares were anticorrelated or uncorrelated (Wijnands 2006; Patruno et al. 2016). Given the lack of *Swift*/XRT data, we therefore look for evidence of reflares primarily in the *Swift*/BAT light curve.

For radio observations D, E, F, the optical and hard X-ray light curves do not show evidence of reflares (with the previously described caveat of possible uncorrelated X-ray/optical behaviour). In addition, observation E was probably carried out at the end of a stable X-ray decay (as shown by the preceding *Swift*/XRT observations, MJD ∼57144 to ∼57148). In observation F, the radio flux density increased by a factor of ≈3 over the 2 d since observation E, with no apparent corresponding increase in the 1–10 keV flux. Unfortunately, the coincidentally large uncertainties in the daily *Swift*/BAT data adjacent to this radio observation were not particularly constraining ($F_{1-10\,\text{keV}} < 10^{-10}$ erg cm^{-2} s^{-1}, 3σ limit, assuming a photon index $\Gamma = 1.8$), so a relatively faint ($L_X < 1.5 \times 10^{35}$ erg s^{-1}), fast X-ray flare without a corresponding optical flare could have been missed. There was also no significant detection in the orbital *Swift*/BAT light curve around observation F. We find it unlikely that the other radio-loud epochs were caused by insufficient sampling of its multiwavelength light curve.

Observations D, E, F, together with previous radio observations, show that SAX J1808.4−3658 can reach quasi-simultaneous radio/X-ray luminosities similar to those of tMSPs. The sparse 1–10 keV sampling around observations D and F could potentially be the reason behind their apparently high radio luminosities, but observation E and that of Gaensler et al. (1999), might require a physical explanation. Below, we investigate possible physical causes.

5.3.2 A collision of the jet with a nearby medium

The enhanced flux during the radio-loud epochs could be caused by additional radio emission from a shock. Thus, a significant fraction of the radio emission could originate from radio lobes or hotspots from the interaction of the jet with the interstellar medium. We do not resolve any extended emission in SAX J1808.4−3658 that might indicate lobes. Based on the size of the synthesized beam at 22 GHz (3.4 arcsec × 0.9 arcsec), we place an upper limit of $\lesssim 2 \times 10^{17}$ cm on the size of the radio source (at a distance of 3.5 kpc). Separations between the two radio lobes produced by outbursting X-ray binaries have been seen to reach similar dimensions (e.g. Bower et al. 2005). Travelling the above distance at velocity c takes 0.2 yr, however. Since this is longer than the outburst time-scale, the reflares cannot be associated with lobes of such size. We cannot dismiss the possibility of smaller radio lobes based on physical size alone. However, the low-density environment of SAX J1808.4−3658 ($N_H = 1.4 \times 10^{21}$ cm^{-2}, inferred from the X-ray spectrum; Pinto et al. 2013) argues against the presence of a dense interstellar medium in its vicinity for a jet to interact with. However, we still cannot rule out the (somewhat unlikely) possibility of a cloud adjacent to the neutron star that does not intervene along our line of sight towards it, which requires a finely tuned geometry.

Instead of the high-density interstellar medium that SAX J1808.4−3658 would need to be embedded in, the jet could interact with a smaller, localized circumbinary structure, produced by accretion/ejection processes in the system, from the current or previous outbursts. Such material would likely lead to accelerated orbital decay (Taam & Spruit 2001). SAX J1808.4−3658, however, undergoes orbital expansion (Patruno et al. 2012), which we take as evidence against the existence of a massive circumbinary structure around the system.

Alternatively, the radio emission could be caused by collisions of a high-velocity collimated jet with slow, wide-angle winds. This scenario is thought to occur in SS433, a black hole system accreting close to the Eddington luminosity, which produces heavy outflows driven by strong radiation pressure (Blundell & Hirst 2011). The coexistence of jets and winds is thought to occur in a few other black hole and neutron star systems at high X-ray luminosities ($L_X \gtrsim 0.3\,L_{Edd}$; Homan et al. 2016). In contrast, SAX J1808.4−3658 only reaches luminosities $L_X \lesssim 0.1\,L_{Edd}$, although it does launch winds (Pinto et al. 2014). If winds are still launched down to $L_X = 10^{33}$ erg s^{-1} (possibly by the propeller mode of accretion; Romanova et al. 2009; Lii et al. 2014), the jet could blow into them, producing the observed radio–X-ray behaviour. In comparison, compact radio and γ-ray emission from cataclysmic variables in outburst originates at the interface between slow and fast outflows (Chomiuk et al. 2014). The possibility of coexisting jets and winds in SAX J1808.4−3658 can be tested in future outbursts with simultaneous radio and high spectral resolution X-ray observations.

Another possibility is that the radio flares are produced by a jet colliding with the accretion disc or the donor star. This could occur if the spin of the neutron star is severely misaligned with respect to the orbit of the donor star, and the accretion disc is warped (Bardeen & Petterson 1975; Maccarone 2002; Butt, Maccarone & Prantzos 2003). If this were the case, we should expect the same mechanism to operate in some black hole systems. The fact that no black hole low-mass X-ray binary in the hard state is known to display as much scatter in the radio/X-ray plane as SAX J1808.4−3658 suggests that such a geometry and emission mechanism are unlikely. In addition, the small donor ($M = 0.03$–$0.06\,M_{\odot}$; Wang et al. 2013),

which covers ≈ 1 per cent of the sky as seen from the neutron star, makes a collision between it and the jet unlikely.

Information about the nature of the radio emission can in principle be gleaned from the spectral index. Radio lobes typically have steep spectral indices ($\alpha \approx -0.7$), similar to discrete, transient jets, whereas steady, compact jets have flat spectra ($\alpha \approx 0$; Blandford & Konigl 1979; Fender 2001). As discussed in Section 4.4.2, the best-constrained spectral index measurement of SAX J1808.4−3658 is $\alpha = -0.24 \pm 0.10$, but we cannot confidently ($<3\sigma$ confidence) favour any emission mechanism, although a flat-spectrum jet during the slow decay is slightly more favourable. The slightly shallower spectral index than expected for neutron stars (with an average $\alpha \approx 0.2$; Russell, Fender & Jonker 2007) could imply contamination from optically thin regions.

Another observational test that would confirm collisions of the jet with a surrounding medium would be a rebrightening in the radio band simultaneous with an increase in optical line flux (e.g. Hα), during a constant, or decaying, optical continuum level (e.g. Gallo et al. 2005).

5.3.3 Collisions within the jet

Shocks within a jet have previously been invoked to explain the radio properties of jets in general (Kaiser, Sunyaev & Spruit 2000; Fender, Belloni & Gallo 2004a; Jamil, Fender & Kaiser 2010; Malzac 2013) and the behaviour of individual X-ray binaries in particular (Fomalont et al. 2001; Ratti et al. 2012). A luminosity-dependent Lorentz factor of the ejecta (invoked by Soleri & Fender 2011 and Russell et al. 2015 to explain the X-ray/radio luminosity tracks of radio-faint black holes) could in principle lead to delayed radio reflares. Fast ejecta launched at the peak of an X-ray reflare could collide with previous slower ejecta, and cause a radio brightening of the source. The typical durations and peak fluxes of the reflares of SAX J1808.4−3658, which are so far unique to this source, might be responsible for the scatter in the radio–X-ray plane that has not been observed in other X-ray binaries.

5.3.4 A large delay between the radio and X-ray emission

The scatter in the radio/X-ray plane could be caused by the rapid variability of SAX J1808.4−3658 and a large delay between the radio and X-ray light curves. In the black hole X-ray binary GX 339−4, infrared emission from the jet lags X-ray emission by 100 ms (Casella et al. 2010); in another black hole system, GRS 1915+105, X-rays lead the radio by ≈ 0.1 h (Mirabel et al. 1998). Such a short time-lag ($\ll 1$ h) cannot explain the radio-loud observations (D, E, F) in SAX J1808.4−3658. A neutron star with a different ejection mechanism (e.g. the propeller mode of accretion/ejection) could potentially show a longer delay between the radio and X-ray bands (of the order of hours). Such a time delay produced by the propeller effect could be common among AMXPs, but it has so far not been detected due to the poor radio sampling of AMXP outbursts.

Still, delays of less than a day would only give a significantly different result for the last radio observation (G), such that its corresponding X-ray flux would be an order of magnitude fainter, making it radio loud.

It could also be that the radio emission is delayed with respect to the X-ray emission by a few days. Given the sparse sampling of the radio light curve, a cross-correlation test for finding the delay between the radio and X-ray emission will not be robust for our data

set. Below, we highlight two possible time delays, but a detailed quantitative analysis will require better sampled multiwavelength light curves.

It is plausible that the radio flare of observation F could actually be produced by the X-ray reflare at MJD $\sim$57144, with a delay of $\sim$5 d. Such long delays have previously been observed between the core and knots in the jet of the neutron star X-ray binary Cir X–1 (Fender et al. 2004c). The knots in the jets of Cir X–1, however, are resolved on 1 arcsec scales, and are likely to be produced during an interaction with the surroundings, which we do not find evidence for in SAX J1808.4−3658 (see Section 5.3.2).

Less likely (as outflows typically follow inflows) is for the radio emission to precede the X-ray emission such that observation F and the reflare at MJD $\gtrsim$ 57152 are directly linked. However, a possible explanation for the radio preceding the X-ray emission could be a time-scale for the diffusion through the magnetosphere that is longer than the ejection time-scale, such that a fraction of an infalling supply of gas is ejected before its remainder penetrates the magnetosphere, as seen in the simulations of Lii et al. (2014).

5.3.5 The ejection of matter in the 'propeller' mode

The radio emission could come from material ejected by the propeller effect, as suggested by Gaensler et al. (1999), who detected the strongest radio emission from SAX J1808.4−3658 a day after the start of the fast X-ray decay during its outburst in 1998. In the propeller mode of accretion, the magnetic pressure of the magnetosphere balances the ram pressure of the infalling matter, accelerating the inner regions of the accretion disc (Illarionov & Sunyaev 1975). If the gas velocity exceeds the escape velocity of the neutron star, outflows are launched from the system (strong propeller). Such outflows prevent most of the disc material from accreting on to the surface of the neutron star, decreasing the radiative efficiency of the flow (Campana & Stella 2000). However, matter may accumulate in the disc, and accrete quasi-periodically on the neutron star even in the strong propeller mode (Lii et al. 2014).

In the case of SAX J1808.4−3658, the propeller effect has been invoked as a possible mechanism behind the rapid X-ray decay during its outbursts (Gilfanov et al. 1998), the re-flares following the main outburst (Patruno et al. 2009, 2016), and the light-curve modulations seen during the main outburst (1–5 Hz; Bult & van der Klis 2014) and reflares (1 Hz; Patruno et al. 2009). This makes it a possible candidate to explain the variable radio emission. At low luminosities, the jet would be dominated by propeller emission, and at higher luminosities it would transition to a jet similar to those of atoll sources. The dipolar and stable magnetic field of SAX J1808.4−3658 (Li et al. 1999) could play a part in the efficient ejection of matter at low accretion rates.

We develop a toy model to explore whether the strong propeller mode of accretion could account for the radio-loud epochs of SAX J1808.4−3658. Given the radio and X-ray properties of tMSPs in the accreting state, in which the propeller is thought to operate (Deller et al. 2015), we expect the kinetic and emission properties of propeller-driven jets to be similar to those of other X-ray binary jets (collimated, flat spectrum). The radio luminosity might therefore be expected to scale with the kinetic power (Heinz & Sunyaev 2003) according to

$$L_{\text{radio}} = L_0 \left(\frac{W_{\text{jet}}}{W_0} \right)^{1.42} . \tag{1}$$

From approximations of the kinetic and radiative powers of the jets of three radio galaxies, Heinz & Grimm (2005) found $W_0 = 6.2 \times 10^{37}$ erg s^{-1}, with an estimated order of magnitude uncertainty, by setting $L_0 = 1.6 \times 10^{30}$ erg s^{-1}, as determined empirically from the Fundamental Plane of accreting black holes (Merloni et al. 2003; Falcke et al. 2004). The large uncertainties come from the difficulty of measuring the kinetic power of jets, and from the orders of magnitude difference between the radiative and kinetic energies of jets.

To estimate the kinetic energy of an outflow, we use energy conservation in the system, which is expressed as

$$\dot{E}_{\text{pot}} + \dot{E}_{\text{sd}} = L_\star + L_{\text{flow}} + W_{\text{jet}} , \tag{2}$$

where $\dot{E}_{\text{pot}}$ is the rate of gravitational potential release, $\dot{E}_{\text{sd}}$ is the spin-down power supplied by the neutron star, $L_\star$ and L_{flow} are the radiated luminosities from the impact stream on to the surface of the neutron star and in the accretion flow, and W_{jet} is the kinetic energy carried by the jet. The total rate of gravitational potential energy release is given by

$$\dot{E}_{\text{pot}} = \frac{GM\dot{M}_{\text{d}}}{R_\star} , \tag{3}$$

where M and $R_\star$ are the mass and radius of the neutron star, respectively.

To estimate the kinetic power flowing into the jet, we use the analysis of D'Angelo et al. (2015, fig. 2) for a 2 ms accreting pulsar with a 10^8 G field, which was based on the numerical work of Ustyugova et al. (2006) and Lii et al. (2014). Their formulation for the radiative efficiency ($\mathcal{F} = (L_{\text{flow}} + L_\star)/\dot{E}_{\text{pot}}$) shows what fraction of the gravitational potential energy is radiated. When the accretion disc truncates below the corotation radius, all matter accretes on to the neutron star, resulting in a radiative efficiency $\mathcal{F} = 1$. At larger truncation radii (set by the magnetospheric radius), matter is redirected into jets, decreasing $\mathcal{F}$ below unity. We can estimate the radiative power of the system as

$$\mathcal{F}\dot{E}_{\text{pot}} = GM\dot{M}_{\text{d}} \left(\frac{1 - f_{\text{out}}}{R_\star} + \frac{1}{2} \frac{f_{\text{out}}}{R_{\text{in}}} \right) \tag{4}$$

(where the factor of 1/2 is from the virial theorem), which we use to estimate the fraction of mass lost to the jet (f_{out}). This assumes that the fraction of radiative power originating from spin-down is negligible. Indeed, we expect less than 1 per cent of the spin-down power to be converted to X-rays (Possenti et al. 2002). To obtain a lower limit for the kinetic power of the jet ($W_{\text{jet}} = 0.5 f_{\text{out}} \dot{M}_d v_{\text{jet}}^2$), we assume matter is ejected at the escape velocity ($v_{\text{jet}} = \sqrt{2GM/R_{\text{in}}}$).

In the propeller regime, the jet draws power from the spin of the neutron star, which in turn loses rotational energy at a rate $\dot{E}_{\text{sd}} = 4\pi^2 I \nu \dot{\nu}$, where I is the moment of inertia of the neutron star ($I = 10^{45}$ g cm^2). We provide an upper limit on the power of the jet by assuming a constant spin-down rate of $\dot{\nu} = 2.5 \times 10^{-14}$ Hz s^{-1} (the upper limit found by Hartman et al. 2008 during outbursts), and that the value of W_0 is one order of magnitude lower than reported by Heinz & Grimm (2005) (who estimate an order of magnitude uncertainty on W_0). When R_{in} is close to the corotation radius, it is expressed as (Spruit & Taam 1993)

$$R_{\text{in}} \approx \left(\frac{\mu^2}{4\Omega\dot{M}_{\text{d}}} \right)^{1/5} , \tag{5}$$

where μ is the magnetic moment of the star ($\mu = BR_\star^2$, where B is the magnetic field strength).

The X-ray luminosity in the 1–10 keV band represents a fraction of the radiative power of the system, such that $L_{\text{X}} = \eta\mathcal{F}\dot{E}_{\text{pot}}$
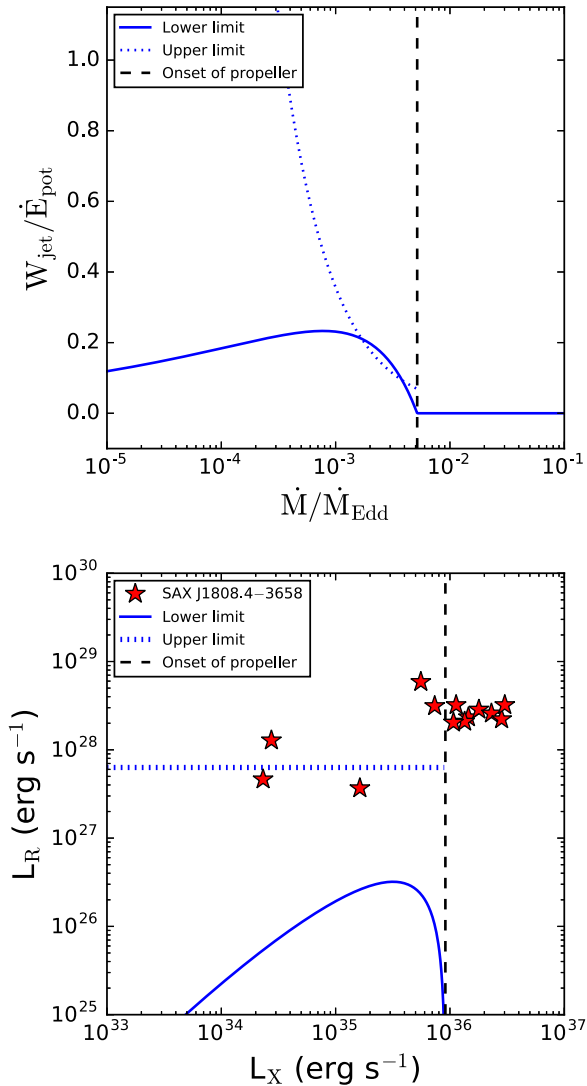
Figure 7. *Top*: Ratio between jet power and gravitational potential energy release, given as a lower limit (continuous line) and upper limit (dotted line). *Bottom*: Radio emission from the strong propeller for our toy model, using the analysis of D'Angelo et al. 2015 (as a lower limit), and using the upper limit on spin-down energy (as an upper limit). The jet is of SAX J1808.4−3658 is unlikely to be caused by a propeller effect described by our model.

($\eta = 0.5$ is the bolometric correction), and the radio luminosity is given by equation (1). Under these assumptions, the inner disc radius is 2.5 times the corotation radius at $L_X = 10^{33}$ erg s^{-1}, making equation (5) valid at the X-ray luminosities sampled here ($L_X = 10^{34}$–10^{37} erg s^{-1}). Fig. 7 (bottom) shows the results of our model. We find that the radio luminosity estimate from the spin-down of the neutron star is compatible with the values derived using the analysis of D'Angelo et al. (2015). The empirical upper limit on the spin-down rate during the outbursts of SAX J1808.4−3658 ($\dot{\nu} < 2.5 \times 10^{-14}$ Hz s^{-1}; Hartman et al. 2008) is also compatible with the maximum spin-down rate in the above model ($\dot{\nu} = 1.7 \times 10^{-14}$ Hz s^{-1}). We find, however, that the radio luminosity predicted by our model is at least one order of magnitude too low for it to account for the behaviour of SAX J1808.4−3658, making it unlikely that the propeller effect is solely responsible for its radio-bright jet. This discrepancy might be explained by a large

fraction of the gravitational potential energy being directed to the jet, or by the poorly known scaling between the power of the jet and radio luminosity, especially in the case of the propeller regime. In addition, simulations show that two kinds of outflows are driven as a consequence of the strong propeller: a slow, matter-dominated disc wind, and a collimated magnetically dominated Poynting jet (Ustyugova et al. 2006; Romanova et al. 2009; Lii et al. 2014). In contrast, our model assumes a jet typical of X-ray binaries, which are often considered to be energetically equipartitioned (not magnetically dominated). Moreover, some X-ray emission is likely to originate at the magnetosphere–disc interface, and the flow is thought to be less radiatively efficient (Papitto & Torres 2015). A full theoretical model that takes into account all these effects and an evolving fraction of ejected mass is beyond the scope of this paper.

To provide more rigorous tests of the connection between propeller outflows and radio luminosity, additional simultaneous radio and X-ray observations of propeller-mode sources are necessary. Focusing on luminosities at which the strong propeller is thought to switch on will assist in quantifying the differences between standard X-ray binary jets and propeller jets. To robustly determine whether propeller outflows are responsible for strong radio emission, an empirical characterization of the connection between the kinetic and radiative signatures of propeller-mode systems is required. Hydrodynamical simulations would be needed to fully explain the observed emission in tMSPs, the radio-loud and radio-faint AMXPs.

5.4 IGR J00291+5934

For the first time, we report a radio–X-ray correlation index β for a neutron star low-mass X-ray binary in the range $L_X \approx 10^{34}$–10^{36} erg s^{-1}, using the detections of IGR J00291+5934. In contrast to SAX J1808.4−3658, IGR J00291+5934 shows correlated decay in the two bands. A correlation slope $\beta = 0.77 \pm 0.18$ in IGR J00291+5934 indicates radiatively inefficient accretion, albeit with weaker radio emission than tMSPs. Different radio–X-ray normalizations have previously been observed between non-pulsating neutron stars (Tetarenko et al. 2016), and a similar behaviour could occur in pulsating neutron stars.

The correlation index is different than measured over the limited $L_X \approx 10^{36}$–10^{37} erg s^{-1} range for the atoll sources in the hard state (Migliari & Fender 2006; Tetarenko et al. 2016). This does not, however, preclude IGR J00291+5934 and some atoll sources from sharing similar radiatively inefficient emission mechanisms, especially since IGR J00291+5934 has a similar radio–X-ray normalization to the atolls 4U 1728–34 and Aql X–1.

The presence of reflares in SAX J1808.4−3658 and lack thereof in IGR J00291+5934 (e.g. Hartman, Galloway & Chakrabarty 2011) highlights additional differences between the two sources. However, as SAX J1808.4−3658 and IGR J00291+5934 are the only two neutron stars with radio coverage in the range $L_X \approx 10^{34}$–10^{36} erg s^{-1}, no firm conclusion can be drawn as to the causes of their different behaviour.

6 CONCLUSIONS

For the first time, multiwavelength observations of SAX J1808.4−3658 and IGR J00291+5934 have allowed us to study the inflow/outflow coupling within individual neutron stars in the $L_X \approx 10^{34}$–10^{36} erg s^{-1} range. We find that SAX J1808.4−3658 is strongly radio-variable and that it does not follow an obvious L_R–L_X relationship, although at the peak of the outburst it has similar radio and X-ray luminosities as

other neutron stars. A combination of factors, such as sparse sampling during the reflares, a long time delay and strong ejections driven by a propeller, are probably responsible for its behaviour. IGR J00291+5934, on the other hand, has a more well-defined radio–X-ray correlation, with $\beta = 0.77 \pm 0.18$. We do not detect IGR J17511−3057, but we place stringent limits on its radio emission. The outburst detections and quiescent non-detection of Cen X−4 are compatible with the radio and X-ray luminosities of other atoll sources. Overall, neutron stars are always at least a factor of five fainter than the radiatively inefficient black hole track (Gallo et al. 2014).

Such varied behaviour across neutron star classes (and even within AMXPs) could be due to the jet launching mechanism, as impacted by the magnetic field and spin of the neutron star. At high X-ray luminosities, where the disc truncates below the corotation radius, there is evidence of different normalizations for each system (Tetarenko et al. 2016). As the mass accretion rate decreases, some systems might enter a strong propeller mode, where matter is ejected more efficiently, increasing the radio flux, possibly contributing to the different correlations seen below $L_X \lesssim 10^{36}$ erg s^{-1}. It is possible, however, that even without the effects of the propeller mode, neutron stars do not follow a unique radio–X-ray relationship and each system might have a unique behaviour, as suggested by Gallo et al. (2014) for black holes.

The varied behaviour of neutron stars at low X-ray luminosities ($L_X \lesssim 0.01 L_{\rm Edd}$) is in contrast to black holes, which seem to all settle on a similar radiatively inefficient track. This emphasizes the need to accumulate more data on neutron stars, rather than black holes, since there seem to be several classes of neutron stars. The difficulty of carrying out these observations due to radio faintness, however, could be addressed by the upcoming next-generation radio interferometers, such as MeerKAT (Jonas 2009) and SKA (Dewdney et al. 2009).

We propose that during its next outburst, SAX J1808.4−3658 should be monitored approximately twice daily for about 3 weeks in the X-ray and radio bands. Such dense sampling during the fast X-ray decay and reflares is essential for tracking the disc–jet coupling in the propeller regime, measuring a radio/X-ray time lag, quantifying the differences in the radio spectra at low and high radio luminosities, and ultimately identifying the mechanism behind the radio emission. Even without a radio detection, Cen X−4 remains a good candidate for future campaigns for testing whether any non-pulsating neutron stars produce jets at the faintest X-ray luminosities ($L_X \approx 10^{32}$ erg s^{-1}).

ACKNOWLEDGEMENTS

REFERENCES

Alpar M. A., Cheng A. F., Ruderman M. A., Shaham J., 1982, Nature, 300, 728
Altamirano D., Watts A., Linares M., Markwardt C. B., Strohmayer T., Patruno A., 2010, MNRAS, 409, 1136
Archibald A. M. et al., 2009, Science, 324, 1411
Archibald A. M. et al., 2015, ApJ, 807, 62
Arnaud K. A., 1996, in Jacoby G. H., Barnes J., eds, ASP Conf. Ser. Vol. 101, Astronomical Data Analysis Software and Systems V. Astron. Soc. Pac., San Francisco, p. 17
Baglio M. C., D'Avanzo P., Muñoz-Darias T., Breton R. P., Campana S., 2013, A&A, 559, A42
Baldovin C. et al., 2009, Astron. Telegram, 2196
Bardeen J. M., Petterson J. A., 1975, ApJ, 195, L65
Bernardini F., Cackett E. M., Brown E. F., D'Angelo C., Degenaar N., Miller J. M., Reynolds M., Wijnands R., 2013, MNRAS, 436, 2465
Bernardini F., Russell D. M., Kolojonen K. I. I., Stella L., Hynes R. I., Corbel S., 2016, ApJ, 826, 149
Bisnovatyi-Kogan G. S., Komberg B. V., 1974, SvA, 18, 217
Blandford R. D., Konigl A., 1979, ApJ, 232, 34
Blandford R. D., Payne D. G., 1982, MNRAS, 199, 883
Blandford R. D., Znajek R. L., 1977, MNRAS, 179, 433
Blundell K. M., Hirst P., 2011, ApJ, 735, L7
Bower G. C., Roberts D. A., Yusef-Zadeh F., Backer D. C., Cotton W. D., Goss W. M., Lang C. C., Lithwick Y., 2005, ApJ, 633, 218
Bozzo E. et al., 2015a, Astron. Telegram, 7275, 1
Bozzo E. et al., 2015b, Astron. Telegram, 7852
Bult P., van der Klis M., 2014, ApJ, 789, 99
Burderi L., Di Salvo T., D'Antona F., Robba N. R., Testa V., 2003, A&A, 404, L43
Burgay M., Burderi L., Possenti A., D'Amico N., Manchester R. N., Lyne A. G., Camilo F., Campana S., 2003, ApJ, 589, 902
Burrows D. N. et al., 2005, Space Sci. Rev., 120, 165
Butt Y. M., Maccarone T. J., Prantzos N., 2003, ApJ, 587, 748
Cackett E. M., Brown E. F., Miller J. M., Wijnands R., 2010, ApJ, 720, 1325
Campana S., Stella L., 2000, ApJ, 541, 849
Campana S., Stella L., Mereghetti S., Cremonesi D., 2000, A&A, 358, 583
Campana S. et al., 2002, ApJ, 575, L15
Campana S., Israel G. L., Stella L., Gastaldello F., Mereghetti S., 2004a, ApJ, 601, 474
Campana S. et al., 2004b, ApJ, 614, L49
Casares J., 2007, in Karas V., Matt G., eds, Proc. IAU Symp. 238, Black Holes from Stars to Galaxies – Across the Range of Masses. Cambridge Univ. Press, Cambridge, p. 3
Casella P. et al., 2010, MNRAS, 404, L21
Chevalier C., Ilovaisky S. A., van Paradijs J., Pedersen H., van der Klis M., 1989, A&A, 210, 114
Chomiuk L. et al., 2014, Nature, 514, 339
Conner J. P., Evans W. D., Belian R. D., 1969, ApJ, 157, L157
Coppejans D. L., Körding E. G., Miller-Jones J. C. A., Rupen M. P., Knigge C., Sivakoff G. R., Groot P. J., 2015, MNRAS, 451, 3801
Corbel S., Fender R. P., Tzioumis A. K., Nowak M., McIntyre V., Durouchoux P., Sood R., 2000, A&A, 359, 251
Corbel S., Koerding E., Kaaret P., 2008, MNRAS, 389, 1697
Corbel S., Coriat M., Brocksopp C., Tzioumis A. K., Fender R. P., Tomsick J. A., Buxton M. M., Bailyn C. D., 2013, MNRAS, 428, 2500
Coriat M. et al., 2011, MNRAS, 414, 677
Cummings J. R., Page K. L., Palmer D. M., Racusin J. L., Siegel M. H., 2015, GCN Circ., 18051

D'Angelo C. R., Fridriksson J. K., Messenger C., Patruno A., 2015, MNRAS, 449, 2803

De Falco V., Kuiper L., Bozzo E., Galloway D. K., Poutanen J., Ferrigno C., Stella L., Falanga M., 2017, A&A, 599, A88

Deller A. T. et al., 2015, ApJ, 809, 13

Dewdney P. E., Hall P. J., Schilizzi R. T., Lazio T. J. L. W., 2009, Proc. IEEE, 97, 1482

Eckert D., Walter R., Kretschmar P., Mas-Hesse M., Palumbo G. G. C., Roques J.-P., Ubertini P., Winkler C., 2004, Astron. Telegram, 352

Elebert P. et al., 2009, MNRAS, 395, 884

Evans W. D., Belian R. D., Conner J. P., 1970, ApJ, 159, L57

Falcke H., Körding E., Markoff S., 2004, A&A, 414, 895

Fender R. P., 2001, MNRAS, 322, 31

Fender R. P., Hendry M. A., 2000, MNRAS, 317, 1

Fender R. P., Gallo E., Jonker P. G., 2003, MNRAS, 343, L99

Fender R. P., Belloni T. M., Gallo E., 2004a, MNRAS, 355, 1105

Fender R., De Bruyn G., Pooley G., Stappers B., 2004b, Astron. Telegram, 361

Fender R., Wu K., Johnston H., Tzioumis T., Jonker P., Spencer R., van der Klis M., 2004c, Nature, 427, 222

Fomalont E. B., Geldzahler B. J., Bradshaw C. F., 2001, ApJ, 553, L27

Gaensler B. M., Stappers B. W., Getts T. J., 1999, ApJ, 522, L117

Gallo E., Fender R. P., Pooley G. G., 2003, MNRAS, 344, 60

Gallo E., Fender R., Kaiser C., Russell D., Morganti R., Oosterloo T., Heinz S., 2005, Nature, 436, 819

Gallo E. et al., 2014, MNRAS, 445, 290

Galloway D. K., Cumming A., 2006, ApJ, 652, 559

Galloway D. K., Markwardt C. B., Morgan E. H., Chakrabarty D., Strohmayer T. E., 2005, ApJ, 622, L45

Gehrels N. et al., 2004, ApJ, 611, 1005

Giles A. B., Hill K. M., Greenhill J. G., 1999, MNRAS, 304, 47

Gilfanov M., Revnivtsev M., Sunyaev R., Churazov E., 1998, A&A, 338, L83

González Hernández J. I., Rebolo R., Peñarrubia J., Casares J., Israelian G., 2005, A&A, 435, 1185

Greenhill J. G., Giles A. B., Coutures C., 2006, MNRAS, 370, 1303

Hartman J. M. et al., 2008, ApJ, 675, 1468

Hartman J. M., Galloway D. K., Chakrabarty D., 2011, ApJ, 726, 26

Heinz S., Grimm H. J., 2005, ApJ, 633, 384

Heinz S., Sunyaev R. A., 2003, MNRAS, 343, L59

Hjellming R. M., 1979, IAU Circ., 3369

Hjellming R. M., Calovini T. A., Han X. H., Cordova F. A., 1988, ApJ, 335, L75

Hjellming R. M., Han X. H., Cordova F. A., Hasinger G., 1990a, A&A, 235, 147

Hjellming R. M. et al., 1990b, ApJ, 365, 681

Holt S. S., 1976, Ap&SS, 42, 123

Homan J., Neilsen J., Allen J. L., Chakrabarty D., Fender R., Fridriksson J. K., Remillard R. A., Schulz N., 2016, ApJ, 830, L5

Iacolina M. N., Burgay M., Burderi L., Possenti A., di Salvo T., 2010, A&A, 519, A13

Illarionov A. F., Sunyaev R. A., 1975, A&A, 39, 185

in 't Zand J. J. M., Heise J., Muller J. M., Bazzano A., Cocchi M., Natalucci L., Ubertini P., 1998, A&A, 331, L25

Jamil O., Fender R. P., Kaiser C. R., 2010, MNRAS, 401, 394

Jonas J. L., 2009, Proc. IEEE, 97, 1522

Jonker P. G., Gallo E., Dhawan V., Rupen M., Fender R. P., Dubus G., 2004, MNRAS, 351, 1359

Jonker P. G., Campana S., Steeghs D., Torres M. A. P., Galloway D. K., Markwardt C. B., Chakrabarty D., Swank J., 2005, MNRAS, 361, 511

Jonker P. G., Torres M. A. P., Steeghs D., 2008, ApJ, 680, 615

Jonker P. G. et al., 2010, MNRAS, 401, 1255

Jonker P. G., Miller-Jones J. C. A., Homan J., Tomsick J., Fender R. P., Kaaret P., Markoff S., Gallo E., 2012, MNRAS, 423, 3308

Jordi K., Grebel E. K., Ammon K., 2006, A&A, 460, 339

Joss P. C., 1977, Nature, 270, 310

Joss P. C., Li F. K., 1980, ApJ, 238, 287

Kaiser C. R., Sunyaev R., Spruit H. C., 2000, A&A, 356, 975

Kaluzienski L. J., Holt S. S., Swank J. H., 1980, ApJ, 241, 779

Kraft R. P., Burrows D. N., Nousek J. A., 1991, ApJ, 374, 344

Kreidberg L., Bailyn C. D., Farr W. M., Kalogera V., 2012, ApJ, 757, 36

Krimm H. A. et al., 2013, ApJS, 209, 14

Kulkarni S. R., Navarro J., Vasisht G., Tanaka Y., Nagase F., 1992, in van den Heuvel E. P. J., Rappaport S. A., eds, X-Ray Binaries and Recycled Pulsars. Kluwer, Dordrecht, p. 99

Lamb F. K., Pethick C. J., Pines D., 1973, ApJ, 184, 271

Lewis F., Roche P., Russell D. M., Fender R. P., 2008, in Bandyopadhyay R. M., Wachter S., Gelino D., Gelino C. R., eds, AIP Conf. Proc. Vol. 1010, A Population Explosion: The Nature & Evolution of X-ray Binaries in Diverse Environments. Am. Inst. Phys., New York, p. 204

Lewis F. et al., 2010, A&A, 517, A72

Li X.-D., Bombaci I., Dey M., Dey J., van den Heuvel E. P. J., 1999, Phys. Rev. Lett., 83, 3776

Lii P. S., Romanova M. M., Ustyugova G. V., Koldoba A. V., Lovelace R. V. E., 2014, MNRAS, 441, 86

Linares M., Tudose V., Migliari S., 2008, Astron. Telegram, 1667

McMullin J. P., Waters B., Schiebel D., Young W., Golap K., 2007, in Shaw R. A., Hill F., Bell D. J., eds, ASP Conf. Ser. Vol. 376, Astronomical Data Analysis Software and Systems XVI. Astron. Soc. Pac., San Francisco, p. 127

Maccarone T. J., 2002, MNRAS, 336, 1371

Malzac J., 2013, MNRAS, 429, L20

Markwardt C. B., Altamirano D., Swank J. H., Strohmayer T. E., Linares M., Pereira D., 2009, Astron. Telegram, 2197

Merloni A., Heinz S., di Matteo T., 2003, MNRAS, 345, 1057

Migliari S., 2011, in Romero G. E., Sunyaev R. A., Belloni T., eds, Proc. IAU Symp. 275, Jets at All Scales. Cambridge University Press, Cambridge, p. 233

Migliari S., Fender R. P., 2006, MNRAS, 366, 79

Migliari S., Fender R. P., Rupen M., Jonker P. G., Klein-Wolt M., Hjellming R. M., van der Klis M., 2003, MNRAS, 342, L67

Migliari S., Fender R. P., Rupen M., Wachter S., Jonker P. G., Homan J., van der Klis M., 2004, MNRAS, 351, 186

Migliari S. et al., 2010, ApJ, 710, 117

Migliari S., Miller-Jones J. C. A., Russell D. M., 2011, MNRAS, 415, 2407

Migliari S., Ghisellini G., Miller-Jones J., Russell D., 2012, Int. J. Mod. Phys. Conf. Ser., 8, 108

Miller-Jones J. C. A., Russell D. M., Migliari S., 2009, Astron. Telegram, 2232

Miller-Jones J. C. A. et al., 2010, ApJ, 716, L109

Mirabel I. F., Rodríguez L. F., 1994, Nature, 371, 46

Mirabel I. F., Dhawan V., Chaty S., Rodriguez L. F., Marti J., Robinson C. R., Swank J., Geballe T., 1998, A&A, 330, L9

Mukai K., 1993, Legacy, 3, 21

Mukherjee D., Bult P., van der Klis M., Bhattacharya D., 2015, MNRAS, 452, 3994

Muno M. P., Remillard R. A., Chakrabarty D., 2002, ApJ, 568, L35

Özel F., Psaltis D., Narayan R., McClintock J. E., 2010, ApJ, 725, 1918

Özel F., Psaltis D., Narayan R., Santos Villarreal A., 2012, ApJ, 757, 55

Paizis A., Nowak M. A., Wilms J., Courvoisier T. J.-L., Ebisawa K., Rodriguez J., Ubertini P., 2005, A&A, 444, 357

Papitto A., Torres D. F., 2015, ApJ, 807, 33

Papitto A., Riggio A., di Salvo T., Burderi L., D'Aì A., Iaria R., Bozzo E., Menna M. T., 2010, MNRAS, 407, 2575

Papitto A. et al., 2013, Nature, 501, 517

Papitto A., de Martino D., Belloni T. M., Burgay M., Pellizzoni A., Possenti A., Torres D. F., 2015, MNRAS, 449, L26

Papitto A., Bozzo E., Sanchez-Fernandez C., Romano P., Torres D. F., Ferrigno C., Kajava J. J. E., Kuulkers E., 2016, A&A, 596, A71

Patruno A., Watts A., Klein Wolt M., Wijnands R., van der Klis M., 2009, ApJ, 707, 1296

Patruno A., Bult P., Gopakumar A., Hartman J. M., Wijnands R., van der Klis M., Chakrabarty D., 2012, ApJ, 746, L27

Patruno A. et al., 2017, ApJ, 841, 98

Patruno A., Maitra D., Curran P. A., D'Angelo C., Fridriksson J. K., Russell D. M., Middleton M., Wijnands R., 2016, ApJ, 817, 100

Penninx W., Lewin W. H. G., Zijlstra A. A., Mitsuda K., van Paradijs J., 1988, Nature, 336, 146

Perley R. A., Chandler C. J., Butler B. J., Wrobel J. M., 2011, ApJ, 739, L1

Pinto C., Kaastra J. S., Costantini E., de Vries C., 2013, A&A, 551, A25

Pinto C., Costantini E., Fabian A. C., Kaastra J. S., in't Zand J. J. M., 2014, A&A, 563, A115

Plotkin R. M. et al., 2017, ApJ, 834, 104

Pooley G., 2004, Astron. Telegram, 355

Possenti A., Cerutti R., Colpi M., Mereghetti S., 2002, A&A, 387, 993

Radhakrishnan V., Srinivasan G., 1982, Curr. Sci., 51, 1096

Ratti E. M. et al., 2012, MNRAS, 423, 2656

Riggio A., Papitto A., Burderi L., di Salvo T., Bachetti M., Iaria R., D'Aì A., Menna M. T., 2011, A&A, 526, A95

Romanova M. M., Ustyugova G. V., Koldoba A. V., Lovelace R. V. E., 2009, MNRAS, 399, 1802

Rupen M. P., Dhawan V., Mioduszewski A. J., Stappers B. W., Gaensler B. M., 2002, IAU Circ., 7997

Rupen M. P., Dhawan V., Mioduszewski A. J., 2004, Astron. Telegram, 364

Rupen M. P., Dhawan V., Mioduszewski A. J., 2005, Astrono. Telegram, 524

Russell D. M., Fender R. P., Jonker P. G., 2007, MNRAS, 379, 1108

Russell T. D. et al., 2015, MNRAS, 450, 1745

Rutledge R., Moore C., Fox D., Lewin W., van Paradijs J., 1998, Astron. Telegram, 8

Sanna A. et al., 2015, Astron. Telegram, 7364, 1

Shaposhnikov N., Titarchuk L., 2006, ApJ, 643, 1098

Shu F., Najita J., Ostriker E., Wilkin F., Ruden S., Lizano S., 1994, ApJ, 429, 781

Soleri P., Fender R., 2011, MNRAS, 413, 2269

Spencer R. E., Rushton A. P., Bałucińska-Church M., Paragi Z., Schulz N. S., Wilms J., Pooley G. G., Church M. J., 2013, MNRAS, 435, L48

Spruit H. C., Taam R. E., 1993, ApJ, 402, 593

Taam R. E., Spruit H. C., 2001, ApJ, 561, 329

Tetarenko A. J. et al., 2016, MNRAS, 460, 345

Torres M. A. P. et al., 2008, ApJ, 672, 1079

Tudose V., Fender R. P., Linares M., Maitra D., van der Klis M., 2009, MNRAS, 400, 2111

Ustyugova G. V., Koldoba A. V., Romanova M. M., Lovelace R. V. E., 2006, ApJ, 646, 304

van Paradijs J., 1998, in Buccheri R., van Paradijs J., Alpar A., eds, NATO Adv. Sci. Inst. Ser. C Vol. 515, The Many Faces of Neutron Stars. Kluwer, Dordrecht, p. 279

Wang Z., Breton R. P., Heinke C. O., Deloye C. J., Zhong J., 2013, ApJ, 765, 151

Wijnands R., 2006, in Lowry J. A., ed., Trends in Pulsar Research. Nova Science Publishers, Inc., New York, NY, USA, p. 53

Wijnands R., van der Klis M., 1998, Nature, 394, 344

Wijnands R., Méndez M., Markwardt C., van der Klis M., Chakrabarty D., Morgan E., 2001, ApJ, 560, 892

This paper has been typeset from a TEX/LATEX file prepared by the author.